Development and Psychopathology **27** (2015), 1555–1576
© Cambridge University Press 2015
doi:10.1017/S0954579415000942

Posterior structural brain volumes differ in maltreated youth with and without chronic posttraumatic stress disorder

MICHAEL D. DE BELLIS,[a] STEPHEN R. HOOPER,[a,b] STEVEN D. CHEN,[a] JAMES M. PROVENZALE,[a] BRIAN D. BOYD,[a] CHRISTOPHER E. GLESSNER,[a] JAMES R. MACFALL,[a] MARTHA E. PAYNE,[a] ROBERT RYBCZYNSKI,[a] AND DONALD P. WOOLLEY[a]

[a]*Duke University School of Medicine; and* [b]*University of North Carolina School of Medicine*

Abstract

Magnetic resonance imaging studies of maltreated children with posttraumatic stress disorder (PTSD) suggest that maltreatment-related PTSD is associated with adverse brain development. Maltreated youth resilient to chronic PTSD were not previously investigated and may elucidate neuromechanisms of the stress diathesis that leads to resilience to chronic PTSD. In this cross-sectional study, anatomical volumetric and corpus callosum diffusion tensor imaging measures were examined using magnetic resonance imaging in maltreated youth with chronic PTSD ($N = 38$), without PTSD ($N = 35$), and nonmaltreated participants ($n = 59$). Groups were sociodemographically similar. Participants underwent assessments for strict inclusion/exclusion criteria and psychopathology. Maltreated youth with PTSD were psychobiologically different from maltreated youth without PTSD and nonmaltreated controls. Maltreated youth with PTSD had smaller posterior cerebral and cerebellar gray matter volumes than did maltreated youth without PTSD and nonmaltreated participants. Cerebral and cerebellar gray matter volumes inversely correlated with PTSD symptoms. Posterior corpus callosum microstructure in pediatric maltreatment-related PTSD differed compared to maltreated youth without PTSD and controls. The group differences remained significant when controlling for psychopathology, numbers of Axis I disorders, and trauma load. Alterations of these posterior brain structures may result from a shared trauma-related mechanism or an inherent vulnerability that mediates the pathway from chronic PTSD to comorbidity.

Abuse and neglect during childhood are grave developmental traumas that are interpersonal, enduring, co-occurring, and associated with high rates of pediatric posttraumatic stress disorder (PTSD; De Bellis & Zisk, 2014). Maltreatment in humans, a social species, is an experience-based unexpected trauma. Magnetic resonance imaging (MRI) studies of medically healthy maltreated children with DSM-IV-TR PTSD and with subthreshold PTSD suggest that maltreatment-related pediatric PTSD is associated with adverse brain development, including smaller cerebral (Carrion et al., 2001; De Bellis et al., 1999, 2002) and cerebellar volumes (De Bellis & Kuchibhatla, 2006), and smaller areas of the cerebellar vermis (Carrion et al., 2009) and corpus callosum (De Bellis et al., 1999, 2002), compared to nonmaltreated youth. Cortical and cerebellar structures and the corpus callosum, a region that contains interhemispheric projections from brain structures involved in the circuits that mediate emotional, behavioral, cognitive, and memory processing, are all implicated in the core processes of intrusion, hopelessness, emotional numbing, and hyperarousal that are dysregulated in PTSD. In these anatomical imaging studies, earlier age of abuse onset, longer abuse duration, and greater PTSD symptoms each were associated with more extreme differences in brain structures when compared to nonmaltreated youth (De Bellis et al., 1999, 2002; De Bellis & Kuchibhatla, 2006). In addition, youth with maltreatment-related PTSD had reduced fractional anisotropy values on diffusion tensor imaging (DTI) brain scans of white matter, indicating less myelin integrity microstructure in the medial and posterior corpus callosum compared to nonmaltreated youth (Jackowski et al., 2008).

However, maltreated youth not assessed for PTSD show evidence of adverse brain development. In a MRI investigation using voxel-based analyses rather than the earlier methods of manual hand tracing of structures, physically abused youth demonstrated multiple clusters of smaller brain areas compared with nonabused youth, especially in orbital frontal cortex, thalamus, parietal, and temporal lobes (Hanson et al., 2010). Pediatric MRI brain investigations of youth who experienced early neglect, and who were not assessed for psychiatric disorders, demonstrated smaller cerebellar volumes (Bauer, Hanson, Pierson, Davidson, & Pollak, 2009). Maltreated youth with higher rates of hyperactivity and conduct problems demonstrated reduced cortical thickness in anterior

We thank the staff of the Healthy Childhood Brain Development Research Program; the individuals who participated in this study; and the following members of the Duke Neuropsychiatric Imaging Research Laboratory: Cynthia R. Key, Denise F. Messer, and Kulpreet Singh for image analysis work. We also thank Richard H. Yaxley for Figure 1. We acknowledge the partial support of this research by Grants K24 MH71434 and K24 DA028773 (to M.D.D.B), R01 MH63407 (to M.D.D.B), R01 AA12479 (to M.D.D.B), and R01 MH61744 (to M.D.D.B).

Address correspondence and reprint requests to: Michael D. De Bellis, Department of Psychiatry and Behavioral Sciences, Duke University Medical Center, Box 104360, Durham, NC 27710; E-mail: michael.debellis@duke.edu.

https://doi.org/10.1017/S0954579415000942 Published online by Cambridge University Press

cingulate, superior frontal gyrus, and orbital frontal cortex, and less surface area in the left middle temporal regions and lingual gyrus than nonmaltreated controls (Kelly et al., 2013). Smaller corpus callosum area measures were reported in an anatomical MRI brain study of neglected children with psychiatric disorders compared to nonmaltreated children with psychiatric disorders (Teicher et al., 2004).

In preclinical studies, maternal deprivation, a model of neglect, increases the death of both neurons and glia cells in cerebral and cerebellar cortices in infant rats (Zhang et al., 2002). Rhesus monkeys raised in individual cages, a model of maternal deprivation, demonstrated decreased corpus callosum size compared with those primates reared in a social environment (Sanchez, Hearn, Do, Rilling, & Herndon, 1998). Primate studies indicated that these adverse effects of early life stress may be caused by stress-induced dysregulation of neurotrophic factors (Cirulli et al., 2009).

Although neuroanatomical studies of adults who were maltreated as children are limited, smaller cerebral volumes have not been reported in adults with maltreatment-related PTSD, unlike in pediatric studies. Adults with PTSD secondary to maltreatment have smaller hippocampal (Thomaes et al., 2010), anterior cingulate (Kitayama, Quinn, & Bremner, 2006; Thomaes et al., 2010), and orbital frontal volumes (Thomaes et al., 2010) compared to adults without maltreatment histories. Similar to pediatric maltreatment-related PTSD studies, smaller areas of the anterior corpus callosum midbody were seen in adult females with child maltreatment-related PTSD compared to adult females without child abuse history or PTSD (Kitayama et al., 2007). Smaller total corpus callosum area was also reported in male and female adults with PTSD compared to controls (Villarreal et al., 2004).

Conversely, healthy adults with maltreatment histories also demonstrated smaller hippocampal (Dannlowski et al., 2012; Teicher, Anderson, & Polcari, 2012), anterior cingulate (Cohen et al., 2006; Dannlowski et al., 2012; van Harmelen et al., 2010), and orbital frontal volumes (Dannlowski et al., 2012). Smaller prefrontal cortex gray matter volumes were seen in adults who experienced severe corporal punishment and did not have PTSD compared with adults without such histories (Tomoda et al., 2009). Smaller anterior corpus callosum volumes were seen in adult patients with bipolar disorder who had a history of child maltreatment compared to patients without maltreatment histories (Bucker et al., 2014).

Complicating brain studies of maltreated individuals are the issues of sex differences and other inherent confounds in maltreatment studies. There are Gender × Maltreatment interactions that occur during brain development (De Bellis et al., 2001). Gender differences in maltreated youth were demonstrated using anatomical MRI (De Bellis & Keshavan, 2003). Maltreated boys and girls with PTSD demonstrated smaller total brain volumes and areas of the posterior corpus callosum (i.e., splenium) compared to nonmaltreated gender matched controls (De Bellis & Keshavan, 2003). Smaller cerebellar volumes were seen in both maltreated boys and girls with PTSD (De Bellis & Kuchibhatla, 2006). However, maltreated boys with PTSD had smaller cerebral volumes, more extensive corpus callosum area differences, and larger lateral ventricular volumes than did control boys; while maltreated girls with PTSD did not show these significant differences compared to control girls, even though both maltreated gender groups had similar traumas, mental health histories, and IQs, suggesting that maltreated males were more vulnerable to the detrimental brain effects of maltreatment-related PTSD compared to maltreated females with PTSD (De Bellis & Keshavan, 2003). In addition, neglect has been shown to have a strong association with smaller corpus callosum size in boys, while sexual abuse was strongly linked to decreased corpus callosum size in girls (Teicher et al., 2004). Moreover, other confounds, such as prenatal substance exposure (Besinger, Garland, Litrownik, & Landsverk, 1999; Kelleher, Chaffin, Hollenberg, & Fischer, 1994; Smith, Johnson, Pears, Fisher, & DeGarmo, 2007), low socioeconomic status (SES; Herrenkohl & Herrenkohl, 2007), youth alcohol and substance use disorders (De Bellis, 2001a), use of psychotropic medications (Raghavan et al., 2005), and medical illnesses (Hussey, Chang, & Kotch, 2006; Leslie et al., 2005), are overrepresented in maltreated youth, which can each independently and negatively influence brain maturation.

Taken together, the existing literature does not clarify whether the brain differences in youth with maltreatment-related PTSD are a consequence of maltreatment or of PTSD, nor does the extant literature consistently address inherent confounds in this field. This is due to the lack of three-cell designs that included maltreated individuals without PTSD as well as nonmaltreated individuals using very strict inclusion and exclusion criteria to address inherent confounds in the field. Given that the research to date does not include maltreated children without PTSD as trauma controls, we do not know if the brain findings reported in maltreated youth were related to PTSD or maltreatment. Therefore, in this cross-sectional investigation, we compared anatomical brain measures and corpus callosum DTI values of maltreated youth with chronic PTSD, maltreated youth resilient to chronic PTSD, and nonmaltreated controls, on measures of cerebral and cerebellar volumes, cortical regional measures, and corpus callosum DTI values, to examine these empirical questions. This study incorporated the use of strict inclusion and exclusion criteria to limit confounds inherent in maltreatment studies. Given our earlier findings of smaller posterior corpus callosum (splenium) and cerebellum volume measures in youth with maltreatment-related PTSD, both of which did not demonstrate Sex × PTSD effects (De Bellis & Keshavan, 2003; De Bellis & Kuchibhatla, 2006), we hypothesized that posterior brain regions (i.e., occipital and posterior parietal cortex, cerebellum volumes, and DTI measures of the posterior corpus callosum) would show differences in maltreated youth with PTSD compared to maltreated youth without PTSD and nonmaltreated youth. Given that sex hormones influence brain development, and the existing data demonstrate sex differences in brain structures in maltreated

https://doi.org/10.1017/S0954579415000942 Published online by Cambridge University Press

youth with PTSD (De Bellis & Keshavan, 2003; Teicher et al., 2004), additional planned analyses of Sex × Group differences were undertaken. Planned comparisons were also undertaken to determine the relationships among these brain structures, PTSD variables, psychopathology, and trauma load.

Method

Subjects

The sample ($n = 132$) consisted of nonmaltreated healthy youth ($n = 59$) and maltreated youth assessed with DSM-IV-TR and DSM-5, resulting in a maltreated without PTSD ($n = 35$) and a PTSD group ($n = 38$) ranging in age from 6 to 16 years. The maltreated groups were defined by a positive forensic investigation conducted by the state Child Protective Services (CPS) that indicated physical or sexual abuse and/or neglect. Maltreated participants were recruited through statewide advertisements targeted at CPS agencies. To reduce selection bias, the study was advertised to CPS statewide, and participants who lived more than 75 miles from the research program were given overnight accommodations. Nonmaltreated healthy volunteers, with no history of DSM Axis I disorders or DSM-IV-TR Type A traumas, recruited from schools and community settings, had a negative maltreatment screen on initial telephone interview. Comprehensive research interviews that indicated any positive history of maltreatment of participants or their siblings, or positive review of pediatric and birth medical records that met state CPS maltreatment criteria, excluded a potential healthy volunteer. Healthy volunteers were recruited to be of similar age, gender, handedness, race, and SES, and their IQ for inclusion was limited to be within one standard error of measure (~3 IQ points; Wechsler, 1991) of the lowest and highest scores of the maltreated youth. Maltreated youth have been shown to have lower IQ scores in both cross-sectional and longitudinal studies; lower IQ is considered a consequence of maltreatment and an inherent confound in maltreatment studies (De Bellis, Hooper, Spratt, & Woolley, 2009; De Bellis, Woolley, & Hooper, 2013; Perez & Widom, 1994). Accordingly, this procedure was used as an attempt to control for this confound. After complete description of the study was given to the legal guardians and participants, written informed consent/assent was obtained to undertake this institutional review board-approved study.

Exclusion criteria were as follows: IQ < 70, chronic medical illness, daily prescription medication, head injury with loss of consciousness, history of traumatic brain injury, neurological disorder, schizophrenia or psychosis, anorexia nervosa, pervasive developmental disorder, obsessive–compulsive disorder, bipolar I disorder or mania, birth weight under 5 lb, severe prenatal (e.g., fetal alcohol and/or drug exposure) or perinatal complications (e.g., neonatal intensive care unit stay), current or lifetime nicotine dependence/alcohol/substance use disorder, contraindications for safe MRI scanning, and Axis I disorder or report of maltreatment that warranted CPS investigation in nonmaltreated controls. Recruitment was challenging because prenatal substance exposure, low SES, alcohol and substance dependence, use of psychotropic medications, and medical illnesses are overrepresented in the maltreated youth population and can independently influence brain maturation in a negative manner. Initial recruitment and scanning begin in 2003 and ended in 2011.

Measures

To examine psychiatric diagnoses and maltreatment characteristics, the Kiddie Schedule for Affective Disorders and Schizophrenia—Present and Lifetime Version (Kaufman et al., 1997) was administered to all caregivers and youth. Because multiple sources of information are needed to gather accurate maltreatment history and related symptoms, we requested and reviewed archival records (e.g., pediatric records, school attendance records, birth records, and forensics records) as additional data sources of mental health, birth history, trauma history, and pediatric health (Kaufman, Jones, Stieglitz, Vitulino, & Mannarino, 1994). If information from these data sources produced evidence meeting any of the exclusionary criteria, the participant was excluded. The Kiddie Schedule for Affective Disorders and Schizophrenia interviewer training and modifications were described previously (De Bellis et al., 2009). Child maltreatment was defined as witnessing domestic violence or experiencing physical, sexual, or emotional abuse and/or neglect that resulted in at least one of the following eight maltreatment categories: witnessing intimate partner violence, physical abuse, sexual abuse, neglect–failure to supervise, neglect–failure to provide, emotional abuse, witnessing or victim of other interpersonal violence, and corporal punishment. Trauma load was defined as the total number of maltreatment categories a youth experienced.

Participants were administered the two-subtest short form (vocabulary and block design) of the Wechsler Intelligence Scale for Children, Third Edition, to obtain an IQ score (Wechsler, 1991). The Child Behavior Checklist (CBCL) was administered to the child's caregiver to measure the child's total internalizing and externalizing behavior problems. Children Global Assessment Scale (CGAS) score (Shaffer et al., 1983) was scored by the interviewer after assessment of all clinical data to provide a continuous measure of child function.

Demographic and behavioral characteristics of the groups

Demographic, clinical, and maltreatment information are reported by group in Tables 1 and 2. The groups were similar in age, gender, handedness, race, weight, height, and SES. Post hoc pairwise group differences revealed that IQ scores were similar in both maltreated groups and significantly lower than controls. The relationships between IQ and PTSD symptoms ($r = .01$, $p = .92$), IQ scores and trauma load ($r = –.15$,

https://doi.org/10.1017/S0954579415000942 Published online by Cambridge University Press

https://doi.org/10.1017/S0954579415000942 Published online by Cambridge University Press

Table 1. *Demographic and clinical characteristics of the study participants*

Variable	Group 1 Healthy Controls ($N = 59$)		Group 2 Maltreated Without PTSD ($N = 35$)		Group 3 Maltreated With PTSD ($N = 38$)		Statistic	p	Pairwise Group Diff.[a]
	Mean (*SD*)	Range	Mean (*SD*)	Range	Mean (*SD*)	Range			
Age (years)	10.8 (2.5)	6.4–16.1	9.8 (2.6)		10.3 (2.6)	6.2–15.7	F (2, 131) = 1.55	.22	
Female/male	33/26		17/18		21/17		$\chi^2 = 0.53$	.77	
Right/left handed	53/6		33/2		34/4		$\chi^2 = 0.66$	.72	
Race: Caus/AA/other	25/26/8		15/14/6		16/19/3		$\chi^2 = 1.67$	.80	
SES	42.4 (13.1)	14–65	38.2 (16.0)		36.6 (13.2)	14–64	F (2, 131) = 2.28	.11	
Weight (lb)	95.0 (37.0)	42–235	89.1 (39.8)	44.5–185	94.3 (46.7)	43–238	F (2, 131) = 9.25	.78	
Height (in.)	57.2 (6.4)	43–73	55.1 (7.3)	43–70	54.8 (6.6)	44–68.5	F (2, 131) = 1.80	.17	
FSIQ	102.1 (11.5)	74–118	93.8 (12.4)	71–115	90.6 (12.4)	71–115	F (2, 131) = 12.0	<.0001	1 > 2, 3
CBCL total score	40.2(8.9)	24–58	55.3 (11.8)	40–83	62.7 (10.4)	43–78	F (2, 131) = 61.7	<.0001	1 < 2 < 3
CBCL internalizing	43.3 (7.9)	33–61	54.3 (10.6)	32–75	60.5 (10.7)	39–79	F (2, 131) = 40.6	<.0001	1 < 2 < 3
CBCL externalizing	41.3 (8.2)	30–62	54.0 (13.1)	33–83	60.5 (11.5)	33–82	F (2, 131) = 40.9	<.0001	1 < 2 < 3
CGAS	89.3 (5.8)	70–98	66.7 (8.9)	50–90	56.0 (8.7)	40–80	F (2, 131) = 240.1	<.0001	1 > 2 > 3

Note: PTSD, Posttraumatic stress disorder; Caus, Caucasian; AA, African American; other, multiracial; SES, socioeconomic status measured by the Hollingshead Four Factor Index; FSIQ, full scale IQ estimated from two factors; CBCL, Child Behavior Checklist total score; CGAS, Children's Global Assessment Scale score.

[a]Comparisons tests for all pairs using Tukey–Kramer honestly significant difference ($q = 2.37$, $p < .05$).

Table 2. *Maltreatment, PTSD symptoms, and diagnostic clinical characteristics of maltreated youth resilient to PTSD and with chronic PTSD*

	Maltreated Without PTSD ($N = 35$)	Maltreated With PTSD ($N = 38$)	Statistic	p
History of Maltreatment Types				
Witnessing intimate partner violence (yes/no)	26/9	32/6	FET	.34
Physical abuse (yes/no)	21/14	31/7	FET	.07
Sexual abuse (yes/no)	7/28	16/22	FET	.05
Neglect				
Failure to supervise (yes/no)	30/5	34/4	FET	.73
Failure to provide (yes/no)	17/18	20/18	FET	1.0
Emotional abuse (yes/no)	15/20	28/10	FET	.01
Witnessing or victim of other personal violence (violent crime; yes/no)	24/11	30/8	FET	.42
Corporal punishment (yes/no)	33/2	36/2	FET	1.0
Mean no. of maltreatment types (8 total), mean ± *SD*	5.2 (1.4)	6.2 (1.3)	F (1, 72) = 8.85	.004
Range	2–8	3–8		
DSM-IV-TR Diagnoses				
PTSD chronic ($n = 38$), mean (*SD*)	—			
Age of onset PTSD (years), mean (*SD*)	—	6.95 (2.5)		
Range		3.0–13.4		
Duration of PTSD (years), mean (*SD*)	—	3.18 (2.4)		
Range		0.25–8.83		
Total PTSD symptoms, mean (*SD*)	3.4 (2.5)	11.1 (2.6)	F (1, 72) = 162.1	<.0001
Range	0–8	5–15		
No. of internalizing disorders, mean (*SD*)	0.20 (0.4)	2.0 (0.9)	F (1, 72) = 17.7	<.0001
Range	0–1	1–4		
Major depression (yes/no)	3/32	16/22	FET	.001
Dysthymia (yes/no)	0/35	7/32	FET	.01
Major depressive disorder NOS (yes/no)	1/34	1/37	FET	1.0
Generalized anxiety disorder (yes/no)	4/31	10/28	FET	.14
Separation anxiety disorder (yes/no)	0/35	5/33	FET	.03
No. of disruptive, mean (*SD*)	0.72 (0.83)	1.3 (1.05)	F (1, 72) = 8.01	.006
Range	0–3	0–3		
ADHD				
Any (yes/no)	17/18	26/12	FET	.10
Combined type (yes/no)	7/28	16/22	FET	<.05
Inattentive type (yes/no)	8/27	6/32	FET	.56
Hyperactive type (yes/no)	1/34	1/37	FET	1.0
NOS (yes/no)	2/33	3/35	FET	1.0
Oppositional defiant disorder (yes/no)	5/30	17/21	FET	.006
Conduct disorder (yes/no)	1/34	6/32	FET	.11
Disruptive behavioral disorder NOS (yes/no)	2/33	2/36	FET	1.0
No. of above Axis I disorders, mean (*SD*)	0.91 (0.95)	3.3 (1.6)	F (1, 72) = 59.0	<.0001
Range	0–3	0–7		
Adjustment disorder with Depressed mood (yes/no)	1/34	0/38	FET	.48
Mixed anxiety and depressed mood (yes/no)	4/31	0/38	FET	.05
Anxiety (yes/no)	8/27	0/38	FET	.002
Total adjustment disorders, mean (*SD*)	0.37 (0.49)	0 (0)	F (1, 72) = 21.8	<.0001
Range	0–1	0–0		

Note: PTSD, Posttraumatic stress disorder; FET, Fisher's exact test; NOS, not otherwise specified; ADHD, attention-deficit/hyperactivity disorder.

$p = .21$), and IQ and number of current Axis I disorders ($r = –.05$, $p = .67$), were not significant. The two maltreatment groups were significantly different from the nonmaltreated group and from each other, with the PTSD group showing the most internalizing and externalizing symptoms on the CBCL, and the lowest levels of global function than the maltreated youth without PTSD, whose symptoms were also significantly lower than the nonmaltreated group.

https://doi.org/10.1017/S0954579415000942 Published online by Cambridge University Press

Maltreated youth with PTSD were more likely to have experienced sexual and emotional abuse, greater trauma load, and exhibit more total Axis I disorders than were the maltreated youth without PTSD. Their PTSD manifestations were both chronic and persistent with a mean duration of 3.18 years. However, both groups of maltreated youth experienced multiple types of severe and enduring maltreatments. Further, the maltreated youth without PTSD had lesser degrees of clinical impairment and were more likely to have a diagnosis of adjustment disorders (with anxiety). Fifteen participants in the maltreated youth without PTSD group had no current Axis I diagnosis, while only five subjects in the PTSD group had chronic PTSD as the sole diagnosis. Four of the maltreated youth without PTSD had met DSM-IV criteria for PTSD in the past but were in complete remission for 12 months prior to this study.

Anatomical acquisitions. Prior to MRI, subjects underwent desensitization with a mock magnetic resonance scanner and were motivated to remain still by allowing them to see their brain images after their scan was completed. No sedation was used. Scanning was supervised by a child psychiatrist (M.D.D.B.). Subjects tolerated the procedure well, and all scans were obtained with minimum head movement artifact.

Images were acquired using the standard circularly polarized head coil on the same Siemens Trio 3.0 Tesla MRI system (Trio, Siemens Medical Systems) running version VA 24 software. The T1-weighted image set was acquired using a three-dimensional axial MPRAGE sequence with repetition time/inversion recovery time/spin echo time = 2300/1100/5.17 ms, flip angle = 8°, a 130 Hz/pixel bandwidth, a 256 × 256 matrix, a 256-mm diameter field of view, 176 slices with a 1-mm slice thickness, and Nex = 1 (no signal averaging), yielding a 1-mm cubic voxel. This pulse sequence was followed by a T2-weighted acquisition using a two-dimensional turbo spin echo pulse sequence with repetition time/spin echo time = 10000/158 ms, turbo factor = 25, a 201 Hz/pixel bandwidth, a 256 × 256 matrix, a 256-mm diameter field of view, 100 slices with a 2-mm slice thickness and Nex = 1 (no signal averaging), and 6/8 partial Fourier acquisition, yielding a 1 × 1 × 2 mm voxel. Next, a proton density-weighted volume was acquired with a two-dimensional turbo spin echo pulse sequence with repetition time/spin echo time = 2780/18 ms, turbo factor = 5, a 201 Hz/pixel bandwidth, a 256 × 256 matrix, a 256-mm diameter field of view, 100 slices with a 2-mm slice thickness and Nex = 1 (no signal averaging), and 6/8 partial Fourier acquisition, yielding a 1 × 1 × 2 mm voxel.

Brain and tissue volumes. All images reported here underwent quality control checks to determine if they were of sufficient quality to process, were reviewed by a neuroradiologist for abnormalities, and were judged to be within the clinical range of normal. Volumetric image analyses were performed in the Neuropsychiatric Imaging Research Laboratory (NIRL). Nonbrain tissue was removed from the T1-weighted images using a two-step process that first applied the Brain Extraction Tool function within the FSL program (Smith, 2002) followed by Brain Surface Extractor from BrainSuite (Sandor & Leahy, 1997; Shattuck & Leahy, 2001; Shattuck, Sandor-Lehy, Schaper, Rottenberg, & Leahy, 2001). If, upon inspection, the nonbrain tissue was not all successfully removed, the resultant skull-stripped T1-weighted images were then registered to the corresponding images from the Cincinnati Children's Hospital Atlas (http://www.irc.cchmc.org/software/pedbrain.php) using the mutual information registration tool from the Insight Toolkit (Yoo et al., 2002). The transformed images were then applied to the original images, completing the coregistration process. The registered images were segmented using expectation maximization segmentation. Expectation maximization segmentation is a fully automated tissue (e.g., gray matter, white matter, cerebrospinal fluid [CSF]) segmentation method originally developed by Dr. Koen Van Leemput at the Katholeike Universiteit Leuven (Maes, Collignon, Vandermeulen, Marchal, & Suetens, 1997; Van Leemput, Maes, Vandermeulen, Colchester, & Suetens, 2001; Van Leemput, Maes, Vandermeulen, & Suetens, 2003) that was optimized for tissue classification in this pediatric study by NIRL. This software program assigns a probability estimate that a given pixel should be classified as gray matter, white matter, CSF, or nonbrain; the resulting brain tissue was measured as the total brain volume. This segmentation was initialized using the pediatric atlas containing prior spatial expectations of each tissue. The tissue probabilities were then derived in an iterative process using the signal intensity distributions of the different tissues for each of the input image contrasts. The process also evaluates and compensates for spatial distributions of intensity that could be due to various MRI artifacts such as radiofrequency inhomogeneity. This method required parameter optimization for each data set due to variations in subjects and scanner upgrades. After identifying the optimal parameters for this pediatric data set, the method was fully automated, which provided an advantage over semiautomated methods that require an analyst to choose seeding points.

Parcellation volumes. Because our primary interest was in the examination of large structures (total cerebral and cerebellar volumes), which were shown to differ in previous studies between the maltreated group with PTSD and nonmaltreated youth (Carrion et al., 2001; De Bellis et al., 1999, 2002; De Bellis & Kuchibhatla, 2006), we did not use voxel-based analyses because these types of analyses assume that a maltreated and a nonmaltreated youth's brain can be equally forced into a standard stereotactic space; if this is not the case, misregistration of anatomical structures and errors can occur (see Giuliani, Calhoun, Pearlson, Francis, & Buchanan, 2005; Kubicki et al., 2002). Our wide age range would also contribute to these types of errors. This factor was extremely important for our analysis decisions because voxel-based analyses remove the global volumes differences in the normalization process; however, determination of global brain differences was our primary study aim. For this reason, we

https://doi.org/10.1017/S0954579415000942 Published online by Cambridge University Press

employed brain parcellation procedures to obtain 16 divisions of regional measures of gray and white matter volume in the cerebrum. This subdivision was performed using the GRID program, which was developed by NIRL. Once the brain was segmented into tissue types and the nonbrain tissue stripped away through a masking procedure, the cerebrum was separated from the cerebellum and brainstem using tracing and connectivity functions. Each scan was realigned to a standard orientation, including making the anterior commissure–posterior commissure plane horizontal. Following this, the planes were defined. A midsagittal plane was used to divide the left and right cerebral hemispheres. Then, an axial plane was created along the anterior commissure–posterior commissure plane, dividing superior regions from inferior. Next, coronal planes were created perpendicular to the axial plane at the anterior and posterior extent of the corpus callosum. Finally, a third coronal plane was created at the midpoint between the first two coronal planes, which divided the brain into anterior and posterior halves in each hemisphere. This procedure is a modification of a procedure previously validated in adults by NIRL (Beyer et al., 2009), and results in a total cerebral volume measure and 16 cerebral parcellation divisions and numbering of regions (Figure 1). Parcellation Regions 1 to 4 reflect the prefrontal cortex; parcellation Regions 5 to 8 include the frontal–parietal cortex and temporal lobe, including the superior frontal–parietal cortex (Regions 6 and 8), temporal poles (Regions 5 and 7), thalamus, amygdala, and basal ganglion areas; parcellation Regions 9 to 12 reflect the parietal–temporal cortex and include pre- and postcentral gyri, supramarginal gyri, posterior cingulate, fornix and superior temporal gyri; and parcellation Regions 13 to 16 reflect the posterior cortex and include the fusiform and lingual gyri, calcarine, precuneus, superior temporal, and occipital regions (Damasio, 1995). Intraclass correlation of interrater reliability for independent designation of regions of segmented cerebral regions obtained from 10 subjects ranged from 0.94 (for left cerebral hemisphere CSF and Region 1 white matter volumes) to 0.99 (for total cerebral volumes and total cerebral gray and white matter volumes, and Regions 5, 7, 8, 9, 10, 11, 12, 14, and 16 gray, white matter, and CSF volumes), and were established prior to data collection.

Cerebellar volumes. Of the larger sample of 132 subjects, we were able to measure cerebellum volumes in 128 subjects; the magnetic resonance scan did not include the entire cerebellum in 4 subjects, who were excluded. This procedure is a modification made by NIRL of a procedure previously validated in youth (De Bellis & Kuchibhatla, 2006; De Bellis et al., 2005). Briefly, following whole-brain tissue segmentation, the cerebrum was masked and applied to the segmented brain, leaving the segmented cerebellum and brain stem. Next, the brain stem and other noncerebellar tissues were masked by tracing out these structures in the sagittal view on the T1-weighted image unless CSF segmentation totally separated brainstem and cerebellum, in which case tracing was done on the segmentation image. The trace began with a medial slice exhibiting the clearest view of the aqueduct of Sylvius, and proceeded laterally through the left and right halves of the brain stem. The cerebellar vellum and peduncles at the anterior surface of the cerebellar hemispheres were ex-

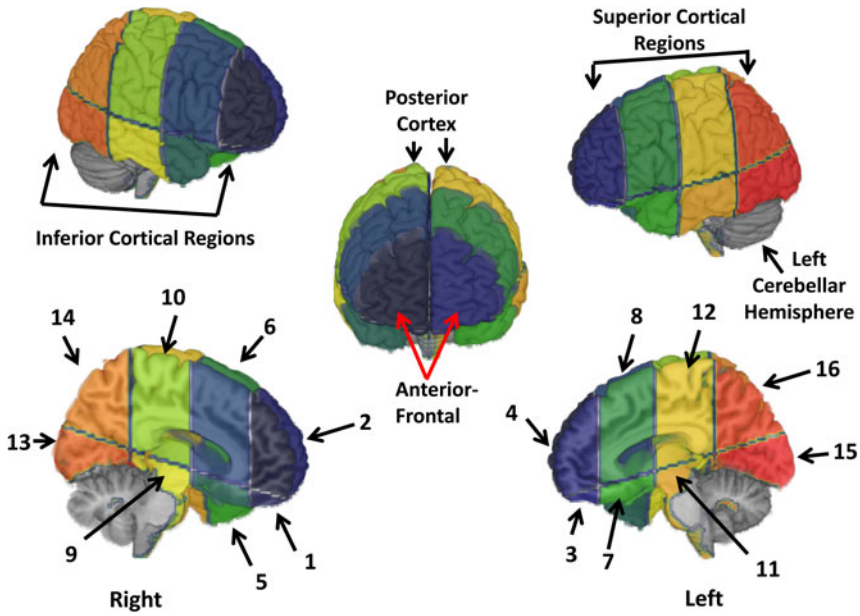


Figure 1. (Color online) This figure illustrates the 16 cerebral parcellation divisions and numbering of regions parcellation Regions 1 to 4 reflect the prefrontal cortex; parcellation Regions 5 to 8 include the frontal–parietal cortex and temporal lobe including the superior frontal–parietal cortex (Regions 6 and 8), temporal poles (Regions 5 and 7), thalamus, amygdala, and basal ganglion areas; parcellation Regions 9 to 12 reflect the parietal–temporal cortex and include pre- and postcentral gyri, supramarginal gyri, posterior cingulate, fornix, and superior temporal gyri; and parcellation Regions 13 to 16 reflect the posterior cortex and include the fusiform and lingual gyri, calcarine, precuneus, superior temporal, and occipital regions.

https://doi.org/10.1017/S0954579415000942 Published online by Cambridge University Press

cluded from the cerebellar volume. The final brain stem tracing was checked with the segmentation image for noncerebellar structures and adjustments made as appropriate. After applying the brain stem mask, tracing of the cerebellar vermis began in an axial image with the most inferior portion of the vermis and proceeded superiorly, excluding the cerebellar tonsil. When the boundary between the vermis and cerebellar hemisphere was unclear, the position of the tracing crosshairs was assessed in coronal and sagittal views. Tracing of the inferior portion of the vermis continued in axial view until the prepyramidal fissure was no longer visible. At that point, the vermis was traced in sagittal view. Two sagittal planes were set as the lateral boundaries for tracing the remaining superior portion of the vermis. These boundaries were set as follows. In an axial view, the most inferior slice exhibiting either superior limb of the cerebellopontine fissure on either side was found and the sagittal slices corresponding to the lateral boundaries of the fourth ventricle determined. These sagittal slices served as candidate vermal boundaries. The boundary slices were adjusted as necessary by inspecting further axial slices in this region to check for their location relative to the apparent ends of the lateral fissures transversing the vermis. In axial view, these fissures run laterally outside the vermis as they angle sharply anteriorly in the cerebellar hemispheres. The final boundaries were fixed to be one voxel lateral to the vermal portion of the medial fissures. Tracing commenced with the left border slice, using the segmented image unless the vermis could not be distinguished from the neighboring cerebellar hemisphere. In that case, the T1-weighted image was used and reference made to coronal and axial views to confirm vermal boundaries. When visible, the superior posterior fissure was followed in tracing the inferior–posterior border of the vermis. No separate volumetric measurements were made for the midbrain, pons, and medulla oblongata.

Following masking of the vermis, the left and right cerebral hemisphere volumes were measured by individually masking each hemisphere using the paint function of ITK-SNAP (Yushkevich et al., 2006). In the axial, T1-weighted image view, the hemispheres were inspected to determine if the left and right hemispheres were separated along a single sagittal plane. If so, each hemisphere was masked via a separate, single operation using the three-dimensional paint function. If not, the two-dimensional paint function was used to mask the left hemisphere slice by slice, followed by masking the right hemisphere with a three-dimensional paint function. A custom MATLAB script was run following the complete masking of the segmented cerebellum to obtain gray and white matter volumes for the vermis and the right and left cerebellar hemisphere volumes. Intraclass correlation of interrater reliability for independent designation of regions of segmented cerebellar regions obtained from 10 subjects ranged from 0.90 (for cerebellar vermis gray matter volume) to 0.99 (for total cerebellar volume, and right and left cerebellar hemisphere gray and white matter volumes), and were established prior to data collection.

MRI acquisition of diffusion-weighted tensor images were acquired using a single-shot echo-planar imaging pulse sequence after anatomical scans. Imaging parameters were echo time = 90 ms, repetition time = 7200 ms, spin bandwidth = 1346 Hz/pixel, and an acquisition matrix of 128 × 64, field of view of 220 mm, and contiguous 3-mm slice thickness. All axial slices were acquired in the axial plane and then reoriented parallel to the anterior commissure–posterior commissure line. Images were acquired with diffusion weighting in each of six different directions, all with a b value (diffusion weighting factor) of 1000. An image with no diffusion weighting ($b = 0$) was acquired as a reference. The set of seven diffusion-weighted images were acquired a total of four times for retrospective averaging to improve image quality and then averaged together after the magnitude-image reconstruction.

Corpus callosum DTI tractography. Of the larger sample of 132 subjects, 79 (nonmaltreated $n = 29$; maltreated without PTSD, $n = 27$; and maltreated with PTSD, $n = 23$) had DTI for which the scan quality was sufficient to undergo DTI tractography. This sample was representative of the larger sample in terms of sociodemographic and IQ measures, except that only right-handed subjects' corpus callosum DTI data was analyzed because of the known differences in DTI measures and handedness (Hagmann et al., 2006). A b_0 correction was performed on the raw diffusion-weighted images using automated image registration in DtiStudio to correct for eddy currents and motion. The fractional anisotropy, apparent diffusion coefficient (ADC), axial diffusivity (λ1, representing the ADC along the fiber direction), and radial diffusivity ([λ2 + λ3]/2 representing ADC perpendicular to the fiber direction) maps were derived via matrix diagonalization of the b_0 corrected diffusion-weighted images in DtiStudio (free software from the Radiology Department, Johns Hopkins University. https://www.dtistudio.org/). The operator was blinded to subject information. We used the fiber assignment by continuous tracking algorithm in DtiStudio 3.0.2 (Jiang and Mori, Baltimore, MD) for tractography. Fractional anistropy thresholds to initiate and continue tracking were set to 0.25; the maximum angle threshold was 70°. Tractography of the corpus callosum was performed by manually drawing regions of interest (ROI) in DtiStudio using a two-ROI approach to derive average DTI metrics along the whole tract of the segmented orbital frontal, anterior frontal, superior frontal, superior parietal, posterior parietal, and occipital regions. One region was drawn on a midsagittal slice encompassing the entire corpus callosum, and six separate ROIs spanning both sides of the midline were used as target regions to segment the corpus callosum into distinct sections. These regions included the orbital–frontal region in which fibers from the orbital–frontal cortex project to the corpus callosum; the anterior frontal region in which fibers from the anterior frontal cortex project to the corpus callosum; the superior frontal region in which fibers from the superior frontal region of the cortex project to the corpus callosum; the superior

https://doi.org/10.1017/S0954579415000942 Published online by Cambridge University Press

parietal region in which fibers from the superior parietal cortex project to the corpus callosum; the posterior parietal region of the corpus callosum in which fibers from the posterior parietal cortex project to the corpus callosum; and the occipital region of the corpus callosum, in which fibers from the occipital cortex project to the corpus callosum. All ROIs were drawn according to specific anatomical landmarks and guidelines based upon a modification of a previously published tract-based corpus callosum segmentation (Lebel, Caverhill-Godkewitch, & Beaulieu, 2010), which was based on the methods of Huang et al. (2005). As seen in Figure 2, one coronal slice was selected at approximately one third of the distance from the genu of the corpus callosum to the most anterior corpus callosum region, and the orbital frontal and anterior frontal-segmented regions were drawn on this slice, and distinguished from each other using an axial slice at the level of the inferior edge of the splenium. The superior frontal and superior parietal-segmented regions were drawn on either side of the central sulcus on the most inferior axial slice on which the central sulcus was still clearly visible. A coronal slice at the edge of the parietal–occipital sulcus was used to draw both the posterior parietal and occipital regions on either side of the parietal–occipital sulcus. We did not measure the temporal region of the corpus callosum due to inability to reliably delineate the tapetum on all the subjects (Figure 2). Regions that included other tracts were used as exclusion areas (e.g., when tracking the anterior frontal region, the orbital frontal region and superior frontal regions were used as exclusion regions). Other exclusion regions were used to eliminate fibers that were not part of the corpus callosum, according to prior anatomical knowledge. This led to tracts identified for each subregion of the corpus callosum (Figure 2) based solely on the medial aspects of the tracts because the lateral corpus callosum projections could not be confidently identified due to the limitations of deterministic tractography in regions of crossing fiber areas. No separate volumetric or area measurements were made for the corpus callosum.

Statistical analysis

General linear models (GLM) were used to examine the hypothesized group effects on brain volumes and DTI measures. The GLM for global volumes included the following covariates that are known to be associated with these brain structural volumes and DTI measures in this pediatric age range: age (Chiang et al., 2011; Giedd & Rapoport, 2010; Lebel & Beaulieu, 2011; Lebel et al., 2010); sex (Asato, Terwilliger, Woo, & Luna, 2010; Chiang et al., 2011; Giedd & Rapoport, 2010); SES (Chiang et al., 2011; De Bellis et al., 1999); IQ (Chiang et al., 2011; Lange, Froimowitz, Bigler, Lainhart, & Brain Development Cooperative Group, 2010); and their interactions with group. The GLM for cortical parcellation volumes covariates included total brain volume (Carrion et al., 2001; De Bellis et al., 1999, 2002; De Bellis & Kuchibhatla, 2006; Giedd & Rapoport, 2010), which differed between groups and is also used as the standard for controlling for variability in brain size with respect to age and sex for pediatric studies (Giedd & Rapoport, 2010; Satterthwaite et al., 2014) and IQ, which differed between the maltreated and nonmaltreated groups, and their interactions. Because of

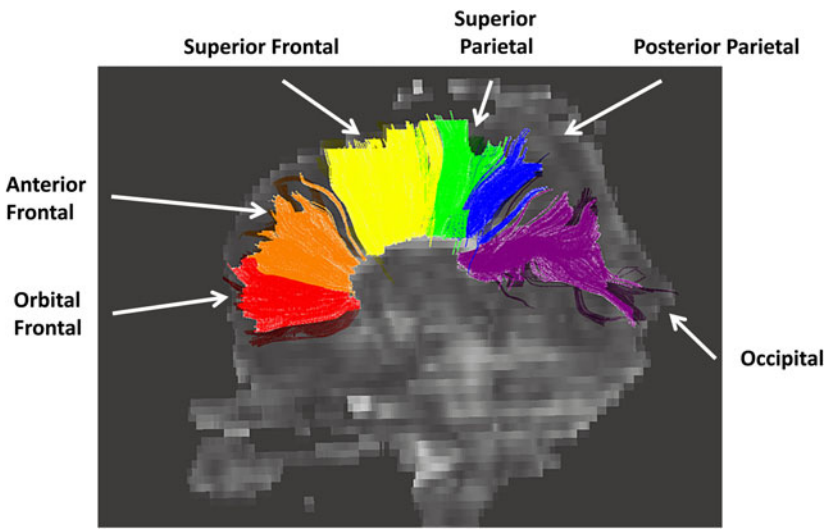


Figure 2. (Color online) This figure illustrates the tractography of the corpus callosum on a fractional anistropy map. These regions included the orbital frontal region in which fibers from the orbital frontal cortex project to the corpus callosum; the anterior frontal region in which fibers from the anterior frontal cortex project to the corpus callosum; the superior frontal region in which fibers from the superior frontal region of the cortex project to the corpus callosum; the superior parietal region in which fibers from the superior parietal cortex project to the corpus callosum; the posterior parietal region of the corpus callosum in which fibers from the posterior parietal cortex project to the corpus callosum; and the occipital region of the corpus callosum, in which fibers from the occipital cortex project to the corpus callosum. All regions of interest were drawn according to specific anatomical landmarks and guidelines based upon a modification of Lebel et al.'s (2010) tract based corpus callosum segmentation, which was based on the methods of Huang et al. (2005).

https://doi.org/10.1017/S0954579415000942 Published online by Cambridge University Press

reports of greater adverse brain development in maltreated males with PSTD than in females with PTSD (De Bellis & Keshavan, 2003), we also undertook planned analyses that controlled for not only total brain volume but also age, sex, SES, IQ, and their interactions with group to examine these effects. We examined the relationships between brain and clinical measures by only including in these correlational analyses the brain measures that were significantly different between groups. Because clinical data were not normally distributed, we used Spearman rho correlations. Our group and clinical comparisons were limited; our hypotheses driven and planned. Therefore, multiple comparison adjustments were not necessary (Rothman, 1990). Alpha was 0.05 (two tailed) and analyses were undertaken using JMP Pro 11 software (SAS Inc.).

Results

Brain volumetry

Group means, standard deviations, and the GLM results are summarized in Table 3. Maltreated children and adolescents with PTSD had smaller cerebral volumes than did maltreated youth without PTSD. Pairwise planned comparisons between groups revealed a trend for smaller total cerebral volumes in the PTSD group compared with controls ($p < .08$). Note the PTSD group showed a moderate effect size for the differences between controls (Cohen $d = \sim 0.61$) and the maltreated group without PTSD (Cohen $d = \sim 0.59$). Compared with controls and maltreated youth without PTSD, maltreated youth with PTSD had smaller total, right, and left hemispheric cerebral gray matter volumes. In addition, maltreated youth with PTSD had smaller cerebellar volumes and smaller total, right, and left hemispheric cerebellar gray matter volumes compared with controls and maltreated youth without PTSD. Furthermore, we separately examined the effects of trauma load, number of current Axis I disorders, and/or CBCL total score on our results; results remained significant ($p \leq .05$) or suggestive ($p \leq .10$) when including these covariates in the GLM. Trauma load and number of current Axis I disorders were not significant predictors of brain volumes in any model. No differences were seen between groups in white matter volumes, cerebellar vermis volume, or CSF volumes.

Cortical parcellation region volumes

Group means, standard deviations, and the GLM results are summarized in Table 4. When controlling for total brain volume and IQ, maltreated youth with PTSD had smaller superior posterior regional gray matter volumes (Regions 14 and 16) than did maltreated youth without PTSD and controls. No other significant differences were seen in cortical gray

Table 3. *Brain volumes in healthy nonmaltreated youth, maltreated youth resilient to PTSD and with chronic PTSD*

Structure (cm^3) (Mean ± *SD*)	Group 1 Healthy Controls ($N = 59$) Mean (*SD*)	Group 2 Maltreated Without PTSD ($N = 35$) Mean (*SD*)	Group 3 Maltreated With PTSD ($N = 38$) Mean (*SD*)	Statistic[a]	*p*	Pairwise Group Diff.[b]
Cerebral volume	1231.2 (138.8)	1223.2 (120.7)	1156.1 (107.1)	F (2, 117) = 4.15	<.02	2 > 3
Cerebral grey matter	719.0 (80.4)	715.3 (71.8)	664.1 (68.9)	F (2, 117) = 5.23	.007	1, 2 > 3
Right cerebral hemisphere grey matter	362.4 (40.4)	360.3 (35.6)	334.7 (34.6)	F (2, 117) = 5.11	<.008	1, 2 > 3
Left cerebral hemisphere grey matter	356.6 (40.25)	354.9 (36.5)	329.4 (34.7)	F (2, 117) = 5.22	<.007	1, 2 > 3
Cerebral white	379.3 (46.4)	379.5 (40.8)	369.2 (39.3)	F (2, 117) = 1.53	.22	
Right cerebral hemisphere white matter	189.0 (23.3)	189.7 (21.1)	183.8 (18.4)	F (2, 117) = 1.88	.16	
Left cerebral hemisphere white matter	190.3 (23.2)	189.0 (19.7)	185.4 (21.1)	F (2, 117) = 1.19	.31	
Cerebral CSF	132.8 (23.0)	128.4 (16.5)	122.8 (15.9)	F (2, 117) = 2.15	.12	
Right cerebral hemisphere CSF	67.5 (11.3)	65.1 (7.9)	62.8 (7.4)	F (2, 117) = 1.57	.21	
Left cerebral hemisphere CSF	65.4 (12.1)	63.35 (8.9)	60.0 (8.9)	F (2, 117) = 2.62	.08	
Cerebellar volume	133.9 (15.4)	135.6 (13.0)	126.4 (8.6)	F (2, 113) = 7.22	.001	1, 2 > 3
Cerebellar volume grey matter	113.2 (13.7)	114.7 (11.6)	106.2 (7.6)	F (2, 113) = 6.74	<.002	1, 2 > 3
Right cerebellar hemisphere grey matter	51.9 (6.5)	51.8 (5.0)	48.7 (4.0)	F (2, 113) = 4.67	<.02	1, 2 > 3
Left cerebellar hemisphere grey	51.3 (6.5)	51.6 (5.0)	48.2 (3.9)	F (2, 113) = 4.38	<.02	1, 2 > 3
Cerebellar volume white matter	20.7 (2.3)	20.8 (2.6)	20.2 (2.75)	F (2, 113) = 2.03	.14	
Right cerebellar hemisphere white matter	9.9 (1.1)	9.9 (1.3)	9.7 (1.5)	F (2, 113) = 1.52	.22	
Left cerebellar hemisphere white matter	10.0 (1.3)	10.2 (1.2)	9.9 (1.5)	F (2, 113) = 1.21	.30	
Cerebellar vermis	10.6 (1.9)	10.9 (1.6)	10.1 (1.1)	F (2, 113) = 2.45	.09	
Cerebellar vermis grey matter	10.0 (1.8)	10.3 (1.5)	9.5 (1.1)	F (2, 113) = 2.51	<.09	
Cerebellar vermis white matter	0.66 (0.22)	0.62 (0.20)	0.60 (0.15)	F (2, 113) = 1.87	.16	

Note: PTSD, Posttraumatic stress disorder; CSF, cerebrospinal fluid.
[a]General linear model examining group, with covariates (age, full scale IQ, socioeconomic status, sex) and their interactions with group.
[b]Least means differences Dunnett Test ($Q = 2.24$, $p \leq .05$).

https://doi.org/10.1017/S0954579415000942 Published online by Cambridge University Press

https://doi.org/10.1017/S0954579415000942 Published online by Cambridge University Press

Table 4. *Cortical parcellation region volumes in healthy nonmaltreated youth and maltreated youth resilient to PTSD and with chronic PTSD*

Structure (cm^3)[a]	Group 1 Healthy Controls ($N = 59$) Mean (*SD*)	Group 2 Maltreated ($N = 35$) Mean (*SD*)	Group 3 Maltreated With PTSD ($N = 38$) Mean (*SD*)	Statistic[b]	*p*	Pairwise Group Diff.[c]	Statistic[d]	*p*	Pairwise Group Diff.[c]
PFC									
Right inferior PFC grey matter Region 1	12.69 (3.41)	12.12 (2.76)	12.73 (3.24)	F (2, 124) = 0.67	.50		F (2, 116) = 1.14	.32	
Right inferior PFC white matter Region 1	3.86 (1.82)	3.80 (1.68)	4.32 (1.20)	F (2, 124) = 1.07	.34		F (2, 116) = 1.14	.32	
Right inferior PFC CSF Region 1	2.56 (0.76)	2.58 (0.88)	2.78 (0.71)	F (2, 124) = 0.89	.41		F (2, 116) = 0.76	.47	
Right superior PFC grey matter Region 2	41.56 (4.81)	41.45 (5.11)	40.99 (5.47)	F (2, 124) = 0.15	.86		F (2, 116) = 0.13	.88	
Right superior PFC white matter Region 2	17.11 (3.01)	17.43 (3.02)	17.72 (3.60)	F (2, 124) = 0.54	.59		F (2, 116) = 0.30	.74	
Right superior PFC CSF Region 2	7.58 (1.85)	7.00 (1.71)	7.51 (1.55)	F (2, 124) = 0.69	.50		F (2, 116) = 0.87	.42	
Left inferior PFC grey matter Region 3	12.15 (3.25)	11.85 (3.18)	11.95 (3.05)	F (2, 124) = 0.20	.82		F (2, 116) = 0.40	.67	
Left inferior PFC white matter Region 3	3.91 (1.84)	3.78 (1.80)	4.31 (2.01)	F (2, 124) = 0.87	.42		F (2, 116) = 0.75	.47	
Left inferior PFC CSF Region 3	2.40 (0.75)	2.55 (0.78)	2.46 (0.69)	F (2, 124) = 0.47	.62		F (2, 116) = 0.38	.68	
Left superior PFC grey matter Region 4	38.27 (4.20)	39.16 (4.58)	37.22 (5.20)	F (2, 124) = 1.60	.21		F (2, 116) = 0.91	.41	
Left superior PFC white matter Region 4	17.63 (2.79)	18.23 (3.04)	18.41 (3.35)	F (2, 124) = 1.07	.34		F (2, 116) = 0.83	.44	
Left superior PFC CSF Region 4	6.75 (1.89)	6.68 (1.94)	6.42 (1.51)	F (2, 124) = 0.28	.76		F (2, 116) = 0.43	.65	
Frontoparietal cortex and temporal pole									
Right inferior grey matter Region 5	37.55 (3.21)	37.18 (3.49)	38.37 (2.56)	F (2, 124) = 1.87	.16		F (2, 116) = 1.34	.26	
Right inferior white matter Region 5	6.54 (1.17)	6.41 (1.13)	6.76 (0.81)	F (2, 124) = 0.92	.40		F (2, 116) = 0.80	.45	
Right inferior CSF Region 5	9.58 (1.28)	9.40 (1.03)	9.76 (0.93)	F (2, 124) = 0.95	.39		F (2, 116) = 0.51	.60	
Right superior grey matter Region 6	62.65 (3.76)	60.82 (4.21)	62.71 (4.22)	F (2, 124) = 1.79	.17		F (2, 116) = 1.24	.29	
Right superior 6 white matter Region 6	6.54 (1.17)	6.41 (1.13)	6.76 (0.81)	F (2, 124) = 2.98	.054	3 > 2	F (2, 116) = 1.77	.18	
Right superior6 CSF Region 6	11.66 (2.07)	10.49 (1.46)	11.88 (1.48)	F (2, 124) = 5.82	<.004	3 > 2	F (2, 116) = 5.43	<.006	1, 3 > 2
Left inferior 6 grey matter Region 7	36.06 (3.37)	35.91 (3.30)	36.54 (2.47)	F (2, 124) = 0.79	.46		F (2, 116) = 0.50	.61	
Left inferior white matter Region 7	6.66 (1.05)	6.38 (1.19)	6.89 (0.90)	F (2, 124) = 1.86	.16		F (2, 116) = 1.54	.22	
Left inferior CSF Region7	9.55 (1.47)	9.63 (0.90)	9.59 (1.09)	F (2, 124) = 0.18	.83		F (2, 116) = 0.27	.76	
Left superior grey matter Region 8	60.40 (3.95)	59.86 (4.10)	59.78 (4.62)	F (2, 124) = 0.19	.83		F (2, 116) = 0.07	.94	
Left superior white matter Region 8	38.23 (3.34)	37.83 (2.80)	39.94 (3.79)	F (2, 124) = 3.24	<.05	3 > 2	F (2, 116) = 2.16	.12	
Left superior CSF Region 8	10.94 (2.73)	10.14 (2.07)	10.57 (1.78)	F (2, 124) = 1.56	.21		F (2, 116) = 1.40	.25	
Parietal temporal cortex									
Right inferior grey matter Region 9	30.87 (2.57)	30.85 (2.48)	31.74 (3.21)	F (2, 124) = 1.12	.33		F (2, 116) = 1.27	.28	
Right inferior white matter Region 9	11.58 (1.37)	11.70 (1.41)	12.05 (1.41)	F (2, 124) = 0.68	.51		F (2, 116) = 1.32	.27	
Right inferior CSF Region 9	6.02 (1.01)	6.23 (1.04)	6.41 (1.52)	F (2, 124) = 0.83	.44		F (2, 116) = 0.44	.64	
Right superior grey matter Region 10	69.75 (5.12)	67.20 (6.55)	67.94 (5.35)	F (2, 124) = 2.57	.08		F (2, 116) = 2.51	<.09	
Right superior white matter Region 10	55.93 (4.75)	55.09 (4.12)	57.43 (4.82)	F (2, 124) = 2.38	.10		F (2, 116) = 1.07	.34	
Right superior CSF Region 10	14.77 (2.80)	13.11 (1.88)	14.54 (1.90)	F (2, 124) = 6.36	.002	2 < 1, 3	F (2, 116) = 5.38	<.006	2 < 1, 3
Left inferior grey matter Region 11	29.93 (2.60)	29.90 (2.20)	30.96 (2.93)	F (2, 124) = 2.45	.09		F (2, 116) = 1.93	.15	
Left inferior white matter Region 11	12.19 (1.52)	12.02 (1.36)	12.57 (1.57)	F (2, 124) = 0.95	.40		F (2, 116) = 0.74	.48	
Left inferior CSF Region 11	6.19 (1.13)	6.62 (1.09)	6.42 (1.48)	F (2, 124) = 0.58	.56		F (2, 116) = 0.74	.48	
Left superior grey matter Region 12	67.83 (5.28)	66.50 (6.23)	65.98 (5.46)	F (2, 124) = 1.97	.14		F (2, 116) = 2.12	.13	
Left superior white matter Region 12	55.97 (10.55)	54.34 (8.58)	57.37 (11.53)	F (2, 124) = 3.22	.04	2 < 3	F (2, 116) = 1.88	.16	
Left superior CSF Region 12	14.01 (3.04)	12.71 (2.43)	13.21 (2.32)	F (2, 124) = 2.68	<.08		F (2, 116) = 2.49	<.09	

https://doi.org/10.1017/S0954579415000942 Published online by Cambridge University Press

Table 4 (*cont.*)

Structure (cm^3)[a]	Group 1 Healthy Controls ($N = 59$) Mean (*SD*)	Group 2 Maltreated ($N = 35$) Mean (*SD*)	Group 3 Maltreated With PTSD ($N = 38$) Mean (*SD*)	Statistic[b]	*p*	Pairwise Group Diff.[c]	Statistic[d]	*p*	Pairwise Group Diff.[c]
Posterior cortex									
Right inferior grey matter Region 13	26.26 (5.30)	28.18 (5.65)	25.87 (4.79)	F (2, 124) = 2.86	.06		F (2, 116) = 1.57	.21	
Right inferior white matter Region 13	10.56 (3.45)	11.51 (3.69)	11.01 (3.31)	F (2, 124) = 0.99	.37		F (2, 116) = 1.11	.33	
Right inferior CSF Region 13	2.94 (0.83)	3.34 (0.66)	3.23 (0.84)	F (2, 124) = 2.87	<.06		F (2, 116) = 2.52	<.09	
Right superior grey matter Region 14	75.44 (7.52)	76.11 (8.45)	71.97 (6.69)	F (2, 124) = 3.83	<.03	1, 2 > 3	F (2, 116) = 2.62	<.08	
Right superior white matter Region 14	41.37 (4.60)	41.91 (5.56)	42.01 (4.81)	F (2, 124) = 0.006	.99		F (2, 116) = 0.06	.94	
Right superior CSF Region 14	11.24 (2.10)	11.08 (2.46)	10.86 (2.07)	F (2, 124) = 0.33	.72		F (2, 116) = 0.53	.59	
Left inferior grey matter Region 15	28.90 (6.64)	29.51 (4.83)	27.63 (4.91)	F (2, 124) = 1.26	.29		F (2, 116) = 0.78	.45	
Left inferior white matter Region 15	11.46 (3.79)	11.92 (3.21)	11.47 (2.98)	F (2, 124) = 0.30	.74		F (2, 116) = 0.34	.71	
Left inferior CSF Region 15	3.00 (0.97)	3.51 (0.80)	3.24 (0.87)	F (2, 124) = 3.92	<.03	2 > 1	F (2, 116) = 3.29	.04	2 > 1
Left superior grey matter Region 16	76.30 (6.75)	76.33 (6.97)	72.40 (6.66)	F (2, 124) = 4.75	.01	1, 2 > 3	F (2, 116) = 4.28	<.02	1, 2 > 3
Left superior white matter Region 16	41.35 (3.85)	41.88 (5.14)	41.91 (6.40)	F (2, 124) = 0.02	.98		F (2, 116) = 0.13	.87	
Left superior CSF Region 16	11.12 (2.28)	10.87 (2.43)	10.90 (2.46)	F (2, 124) = 1.95	.15		F (2, 116) = 3.73	<.03	1, 2 > 3

Note: PTSD, Posttraumatic stress disorder; PFC, prefrontal cortex; CSF, cerebrospinal fluid.
[a]Adjusted for total brain volume.
[b]General linear model examining group, with covariates: total brain volume, full scale IQ, and interactions.
[c]Least means differences Dunnett Test ($Q = 2.24$, $p \leq .05$).
[d]General linear model examining group with total brain volume, and covariates: age, full scale IQ, socioeconomic status, sex, and their interactions with group.

matter regions. Maltreated children and adolescents with PTSD showed larger white matter volumes in the right (Region 6) and left (Region 8) superior frontal–parietal cortex compared with maltreated youth without PTSD; and pairwise planned comparisons between groups revealed a trend for larger white matter in these regions in the PTSD group compared with controls ($p < .09$ and $= .10$, respectively). Maltreated children and adolescents with PTSD showed larger white matter volume in the left superior parietal–temporal cortex (Region 12) compared with maltreated youth without PTSD. No other significant differences were seen in cortical white matter regions.

Maltreated children and adolescents with PTSD showed larger CSF volumes in the right superior parietal–temporal cortex Regions 6 and 10 compared with maltreated youth without PTSD. Nonmaltreated youth also showed significantly greater CSF in the right superior parietal–temporal cortex Region 10 compared with maltreated youth without PTSD. Maltreated children and adolescents without PTSD had larger CSF volumes in the left inferior posterior cortex Region 15 compared to controls. No other significant differences were seen in cortical CSF volumes.

We performed additional GLM to examine the effects of Sex × Group in which we controlled for age, sex, SES, IQ, and their interactions (Table 4). Except for the findings of right (Region 6) and left (Region 8) superior frontal–parietal cortex white matter and left superior parietal cortex white matter (Region 12), all results survived the analyses that controlled for age, sex, SES, IQ, and their interactions. Smaller right superior posterior cortex gray matter (Region 14) showed a trend for group differences ($p < .08$). However, the pairwise comparison was significant for the PTSD group to show less gray matter in this region than for controls ($p < .05$). An additional result of significantly less CSF in the left superior posterior cortex CSF in Region 16 in the maltreated group with PTSD compared to the other two groups was uncovered. Less CSF means less brain tissue in this region and is in accord with the overall finding of less gray matter in PTSD in Region 16.

There was one significant Sex × Group interaction in that maltreated males with and without PTSD showed less gray matter in left superior prefrontal cortex (Region 4) compared to maltreated females with and without PTSD ($F = 4.16$, $p < .02$; LS means differences Dunnett test for both pairwise comparisons were $p < .01$; Figure 3). A trend for maltreated males with PTSD to show less left superior prefrontal cortex gray matter (Region 4) than male controls ($p < .08$) was seen.

In these analyses, we separately examined the effects of trauma load, number of current Axis I disorders, and/or CBCL total score on our results; results remained significant ($p \leq .05$) or suggestive ($p \leq .10$) when including these covariates in the GLM. Trauma load was not a significant predictor of brain volumes in any of the models, except for gray matter volume in Region 16 ($F = 4.30$, $p = .04$). Number of

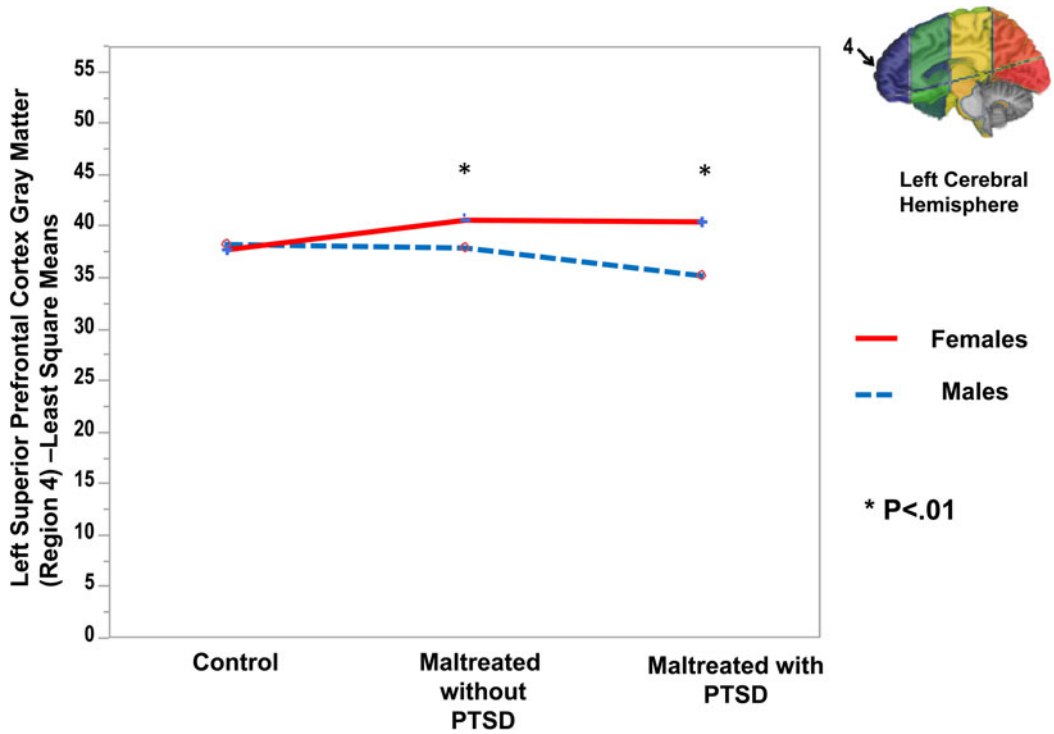


Figure 3. (Color online) Maltreated males with and without posttraumatic stress disorder (PTSD) showed less gray matter in the left superior prefrontal cortex gray matter (Region 4 inset) compared to maltreated females with and without PTSD ($F = 4.16$, $p < .02$; LS means differences Dunnett test for both pairwise comparisons were $p < .01$). There was a trend for maltreated males with PTSD to show less left superior prefrontal cortex gray matter (Region 4) than did male controls ($p < .08$).

https://doi.org/10.1017/S0954579415000942 Published online by Cambridge University Press

Axis I disorders was not a significant predictor of brain volumes in any of the models, except for left superior white matter in Region 8 ($F = 7.01$, $p < .01$) and in Region 10 ($F = 7.61$, $p < .01$), and gray matter in posterior cortex Region 16 ($F = 4.52$, $p < .04$).

Corpus callosum DTI tractography measures

Maltreated children and adolescents with PTSD had lower axial diffusivity mean tractography values in the occipital region that project to the splenium of the corpus callosum than did maltreated youth without PTSD and controls (Table 5). We separately examined the effects of trauma load, number of current Axis I disorders, and/or CBCL total score on our axial diffusivity values; results remained significant ($p \leq .05$) or suggestive ($p \leq .10$) when including these covariates in the GLM. No other significant differences were seen between groups with regard to any of the other corpus callosum DTI values.

Relationships between brain and clinical measures

In maltreated youth, a greater number of PTSD symptoms significantly and negatively correlated with smaller cerebral volume, cerebral gray matter, right and left cerebral hemisphere gray matter, cerebellar gray matter, right and left cerebellar hemisphere gray matter, right (Region 14) and left (Region 16) superior occipital cortex gray matter volumes, and left (Region 16) superior CSF volumes as well as axial diffusivity in occipital region (Table 6). Greater number of current DSM-TR Axis I disorders, higher CBCL total, and higher CBCL externalizing scores significantly and negatively correlated with smaller cerebellar and cerebellar gray matter volumes. Higher level of function (CGAS score) was significantly and positively correlated with greater cerebellar volumes and axial diffusivity in the occipital region. Left inferior CSF Region 15 was significantly and positively correlated with higher CBCL total, CBCL internalizing, and CBCL externalizing scores. No other significant relationships were seen between clinical and brain variables (Table 6). No significant correlations were seen between any of the brain measures and PTSD age of onset or PTSD duration.

Discussion

To the best of our knowledge, our study is the first to examine brain differences in global brain volumes in maltreated children and adolescents with and without chronic PTSD. Medically healthy and comprehensively assessed children and adolescents with the diagnosis of maltreatment-related PTSD had smaller cerebral and cerebellar gray matter volumes than maltreated youth without PTSD and sociodemographically similar nonmaltreated control subjects. Furthermore, youth with pediatric maltreatment-related PTSD had less gray matter in the posterior superior cortical regions that include brain regions critical for language, vision, visual–spatial skills, emotional and behavioral regulation, and higher order cognitive processes (e.g., fusiform and lingual gyri, calcarine, precuneus, superior temporal, and occipital cortex and cerebellum), than did maltreated youth without PTSD and sociodemographically similar, nonmaltreated control subjects. As seen in earlier studies of maltreated youth with PTSD (De Bellis et al., 1999, 2002), in this study, total cerebral and cerebellar volumes significantly and negatively correlated with greater number of PTSD symptoms in maltreated youth. This study also demonstrated differences in the microstructure (axial diffusivity) of the corpus callosum fibers that project to occipital region of the posterior cortex in youth with pediatric maltreatment-related PTSD compared to maltreated youth without PTSD and controls.

Maltreated youth with PTSD were psychobiologically different from maltreated youth without PTSD and nonmaltreated controls. The PTSD group suffered from a greater number of types of maltreatment and was more likely to have been sexually and emotionally abused than maltreated youth without PTSD. The PTSD group also suffered a greater number of current lifetime disorders along the internalizing and externalizing spectrums than did maltreated youth without PTSD. Although maltreated youth with PTSD had greater psychopathology, numbers of Axis I disorders, and trauma load, the group differences remained significant or near significant when controlling for these factors. This work furthers our previous studies that found smaller cerebral and cerebellar volumes in pediatric maltreatment-related PTSD but did not control for maltreatment without PTSD (De Bellis et al., 1999, 2002; De Bellis & Kuchibhatla, 2006), by demonstrating that maltreated children and adolescents with chronic PTSD have evidence of adverse brain development compared to maltreated youth resilient to chronic PTSD and nonmaltreated youth.

Smaller posterior cortex and cerebellar gray matter volumes may result from shared trauma mechanisms or a vulnerability to PTSD symptoms that mediates the pathway from chronic PTSD to comorbidity. Maltreated-related PTSD is a complex disorder that occurs after a traumatic event. The cluster symptoms of intrusive reexperiencing of the trauma(s), persistent avoidance of stimuli associated with the trauma(s), emotional numbing and dissociation, and persistent symptoms of increased physiological arousal are each associated with dysregulation of at least one major biological stress system as well as several different brain circuits involved in behavioral, cognitive, and emotional regulation (De Bellis & Zisk, 2014). These affected posterior cortical regions contain the fusiform and the lingual gyri, which are involved in the recognition of faces (Prochnowa et al., 2013), language, and identification of meaningful objects (Devlin, Jamison, Gonnerman, & Matthews, 2006). Regions 14 and 16 also contain the precuneus, which has widespread connections to frontal and parietal cortices and subcortical structures and is involved in highly integrated tasks, including visual–spatial imagery, episodic memory retrieval, and self-processing operations (i.e., interlinking personal identity and past personal experiences, and an awareness of one's self; Cavanna & Trimble, 2006). Regions 14 and

https://doi.org/10.1017/S0954579415000942 Published online by Cambridge University Press

Table 5. *Corpus callosum diffusion tensor imaging tractography*

	Group 1 Healthy Controls ($N = 29$)	Group 2 Maltreated Without PTSD ($N = 27$)	Group 3 Maltreated With PTSD ($N = 23$)	Statistic[a]	p	Pairwise Group Diff.[b]
Orbital frontal region						
FA	0.476 (0.032)	0.473 (0.021)	0.466 (0.030)	F (2, 64) = 0.19	.83	
ADC	0.000966 (0.000045)	0.000977 (0.000035)	0.000968 (0.000047)	F (2, 64) = 0.22	.80	
Axial diffusivity	0.001538 (0.000081)	0.001555 (0.000054)	0.001528 (0.000055)	F (2, 64) = 0.66	.52	
Lambda 2	0.000806 (0.000045)	0.000813 (0.000039)	0.000811 (0.000056)	F (2, 64) = 0.38	.69	
Lambda 3	0.000575 (0.000047)	0.000585 (0.000036)	0.000586 (0.000051)	F (2, 64) = 0.04	.96	
Radial diffusivity	0.000690 (0.000044)	0.000699 (0.000035)	0.000699 (0.000052)	F (2, 64) = 0.05	.95	
Anterior frontal region						
FA	0.451 (0.032)	0.462 (0.024)	0.451 (0.033)	F (2, 64) = 1.10	.34	
ADC	0.000951 (0.000050)	0.000952 (0.000037)	0.000947 (0.000045)	F (2, 64) = 0.23	.79	
Axial diffusivity	0.001480 (0.000066)	0.001498 (0.000065)	0.001474 (0.000064)	F (2, 64) = 0.05	.95	
Lambda 2	0.000812 (0.000053)	0.000805 (0.000039)	0.000804 (0.000051)	F (2, 64) = 0.73	.48	
Lambda 3	0.000580 (0.000057)	0.000573 (0.000033)	0.000582 (0.000050)	F (2, 64) = 0.64	.53	
Radial diffusivity	0.000696 (0.000053)	0.000689 (0.000035)	0.000693 (0.000050)	F (2, 64) = 0.62	.54	
Superior frontal region						
FA	0.495 (0.035)	0.492 (0.024)	0.489 (0.037)	F (2, 64) = 0.23	.79	
ADC	0.000883 (0.000052)	0.000910 (0.000040)	0.000892 (0.000033)	F (2, 64) = 1.24	.29	
Axial diffusivity	0.001424 (0.000058)	0.001466 (0.000064)	0.001432 (0.000047)	F (2, 64) = 2.77	.07	
Lambda 2	0.000731 (0.000065)	0.000756 (0.000046)	0.000743 (0.000050)	F (2, 64) = 0.47	.63	
Lambda 3	0.000506 (0.000056)	0.000522 (0.000036)	0.000517 (0.000043)	F (2, 64) = 0.06	.94	
Radial diffusivity	0.000618 (0.000060)	0.000639 (0.000039)	0.000630 (0.000045)	F (2, 64) = 0.23	.79	
Superior parietal region						
FA	0.481 (0.041)	0.475 (0.040)	0.477 (0.035)	F (2, 64) = 0.27	.76	
ADC	0.000925 (0.000069)	0.000957 (0.000066)	0.000946 (0.000063)	F (2, 64) = 0.19	.83	
Axial diffusivity	0.001481 (0.000094)	0.001524 (0.000104)	0.001506 (0.000098)	F (2, 64) = 0.51	.60	
Lambda 2	0.000765 (0.000081)	0.000800 (0.000067)	0.000784 (0.000066)	F (2, 64) = 0.23	.80	
Lambda 3	0.000541 (0.000064)	0.000562 (0.000067)	0.000560 (0.000053)	F (2, 64) = 0.06	.94	
Radial diffusivity	0.000653 (0.000071)	0.000681 (0.000065)	0.000672 (0.000059)	F (2, 64) = 0.02	.98	
Posterior parietal region						
FA	0.472 (0.035)	0.468181 (0.030)	0.460452 (0.041)	F (2, 64) = 0.40	.67	
ADC	0.000925 (0.000051)	0.000950 (0.000061)	0.000929 (0.000046)	F (2, 64) = 0.12	.89	
Axial diffusivity	0.001474 (0.000072)	0.001508 (0.000088)	0.001462 (0.000087)	F (2, 64) = 0.59	.56	
Lambda 2	0.000759 (0.000055)	0.000783 (0.000063)	0.000770 (0.000059)	F (2, 64) = 0.03	.97	
Lambda 3	0.000552 (0.000053)	0.000572 (0.000056)	0.000566 (0.000046)	F (2, 64) = 0.11	.90	
Radial diffusivity	0.000656 (0.000053)	0.000678 (0.000058)	0.000668 (0.000052)	F (2, 64) = 0.02	.98	
Occipital region						
FA	0.490 (0.031)	0.487 (0.028)	0.484 (0.030)	F (2, 64) = 0.05	.95	
ADC	0.001017 (0.000074)	0.001022 (0.000053)	0.000992 (0.000062)	F (2, 64) = 2.46	.09	
Axial diffusivity	0.001642 (0.000095)	0.001649 (0.000080)	0.001594 (0.000074)	F (2, 64) = 2.72	<.03	1, 2 > 3
Lambda 2	0.000818 (0.000071)	0.000824 (0.000060)	0.000801 (0.000069)	F (2, 64) = 1.09	.34	
Lambda 3	0.000609 (0.000073)	0.000614 (0.000048)	0.000596 (0.000061)	F (2, 64) = 1.17	.32	
Radial diffusivity	0.000713 (0.000071)	0.000719 (0.000051)	0.000699 (0.000064)	F (2, 64) = 1.18	.31	

Note: PTSD, Posttraumatic stress disorder; FA, fractional anisotropy; ADC, apparent diffusion coefficient.
[a]General linear model examining group, with covariates: age, full scale IQ, socioeconomic status, sex, and their interactions with group.
[b]Least means differences Dunnett Test, Q = 2.24, $p \leq .05$.

16 include the calcarine component of the occipital cortex, which is involved in primary, secondary, and tertiary visual complex functions (Dougherty et al., 2003; Isabelle, Paradis, Kosslyn, & Denis Le Bihan, 2000; Solomon & Rosa, 2014). The cerebellum is a complex brain structure involved in cognitive functions (Riva & Giorgi, 2000), decision making, reward circuits, and new learning (Bellebaum & Daum, 2007; Thoma, Bellebaum, Koch, Schwar, & Daum, 2008), and the default mode or resting state network, which is associated with understanding social intentions (Fransson, 2006). The cerebellum is also involved in emotional processing and fear conditioning (Sacchetti, Scelfo, Tempia, & Strata, 2004; Schutter & van Honk, 2005; Sehlmeyer et al., 2009). Based on operant conditioning theory, PTSD is considered a disorder of recovery, where individuals who suffer from trauma fail to learn extinction and extinction retention of the fear response elicited by traumatic reminders (Pitman et al., 2012; Yehuda & LeDoux, 2007). Thus, less gray matter volume in the posterior brain regions is likely involved in this complex disorder where traumatic reminders are social in nature. Our

https://doi.org/10.1017/S0954579415000942 Published online by Cambridge University Press

Table 6. *Spearman rho correlations between brain and clinical measures*

Brain Measures	CBCL Total Score	CBCL Internalizing	CBCL Externalizing	CGAS	No. of Maltreatment Types	No. of PTSD Symptoms	No. of Axis I Disorders
Cerebral volume	−0.03 ($p = .78$)	0.01 ($p = .95$)	−0.03 ($p = .80$)	0.14 ($p = .22$)	0.00 ($p = .99$)	−0.31 ($p < .02$)	−0.21 ($p = .07$)
Cerebral grey matter	−0.02 ($p = .85$)	−0.01 ($p = .91$)	−0.04 ($p = .72$)	0.13 ($p = .27$)	−0.01 ($p = .92$)	−0.33 ($p = .007$)	−0.21 ($p < .07$)
Right cerebral hemisphere grey matter	−0.035 ($p = .77$)	−0.03 ($p = .82$)	−0.05 ($p = .68$)	0.14 ($p = .24$)	−0.005 ($p = .97$)	−0.32 ($p < .01$)	−0.22 ($p < .06$)
Left cerebral hemisphere grey matter	−0.01 ($p = .91$)	−0.01 ($p = .97$)	−0.03 ($p = .78$)	0.12 ($p = .30$)	−0.01 ($p = .92$)	−0.34 ($p < .006$)	−0.20 ($p < .10$)
Cerebellar volume	−0.27 ($p < .03$)	−0.15 ($p = .23$)	−0.29 ($p < .02$)	0.25 ($p < .04$)	−0.17 ($p = .17$)	−0.45 ($p = .0002$)	−0.32 ($p = .006$)
Cerebellar volume grey matter	−0.25 ($p < .04$)	−0.13 ($p = .27$)	−0.29 ($p = .01$)	0.22 ($p = .06$)	−0.145 ($p = .23$)	−0.43 ($p = .0004$)	−0.27 ($p = .02$)
Right cerebellar hemisphere grey matter	−0.15 ($p = .24$)	−0.05 ($p = .72$)	−0.20 ($p = .12$)	0.13 ($p = .31$)	−0.11 ($p = .38$)	−0.38 ($p < .005$)	−0.18 ($p = .16$)
Left cerebellar hemisphere grey	−0.18 ($p = .16$)	−0.08 ($p = .51$)	−0.21 ($p = .09$)	0.18 ($p = .17$)	0.09 ($p = .49$)	−0.39 ($p = .003$)	−0.23 ($p < .08$)
Right superior 6 white matter Region 6	−0.12 ($p = .32$)	−0.14 ($p = .21$)	−0.09 ($p = .45$)	0.01 ($p = .92$)	−0.05 ($p = .64$)	−0.03 ($p = .79$)	−0.08 ($p = .52$)
Right superior CSF Region 6	0.007 ($p = .95$)	0.003 ($p = .98$)	0.009 ($p = .94$)	0.06 ($p = .62$)	−0.16 ($p = .16$)	0.18 ($p = .14$)	0.15 ($p = .21$)
Left superior white matter Region 8	−0.16 ($p = .19$)	−0.16 ($p = .18$)	−0.12 ($p = .31$)	0.06 ($p = .62$)	−0.02 ($p = .86$)	−0.04 ($p = .73$)	−0.15 ($p = .21$)
Right superior CSF Region 10	0.08 ($p = .48$)	0.17 ($p = .14$)	0.015 ($p = .90$)	0.01 ($p = .92$)	0.04 ($p = .75$)	0.15 ($p = .22$)	0.02 ($p = .84$)
Left superior white matter Region 12	−0.10 ($p = .39$)	−0.05 ($p = .66$)	−0.04 ($p = .74$)	0.05 ($p = .67$)	−0.01 ($p = .91$)	−0.01 ($p = .94$)	−0.11 ($p = .34$)
Right superior grey matter Region 14	0.05 ($p = .66$)	0.10 ($p = .40$)	0.04 ($p = .74$)	0.12 ($p = .32$)	0.03 ($p = .77$)	−0.38 ($p < .002$)	−0.17 ($p = .16$)
Left inferior CSF Region 15	0.26 ($p < .03$)	0.24 ($p < .04$)	0.26 ($p < .03$)	0.15 ($p = .19$)	−0.17 ($p = .14$)	−0.22 ($p = .08$)	−0.06 ($p = .62$)
Left superior grey matter Region 16	0.07 ($p = .55$)	0.10 ($p = .38$)	0.07 ($p = .56$)	0.10 ($p = .39$)	0.08 ($p = .50$)	−0.35 ($p < .005$)	−0.15 ($p = .21$)
Left superior CSF Region 16	0.17 ($p = .16$)	0.22 ($p < .07$)	0.19 ($p = .11$)	0.15 ($p = .21$)	0.07 ($p = .58$)	−0.30 ($p < .02$)	−0.10 ($p = .39$)
DTI occipital region Axial diffusivity	0.07 ($p = .61$)	−0.05 ($p = .73$)	−0.10 ($p = .49$)	0.33 ($p < .03$)	−0.12 ($p = .39$)	−0.29 ($p < .05$)	−0.17 ($p = .25$)

Note: CBCL, Child Behavior checklist total score; CGAS, Children's Global Assessment Scale Score; PTSD, posttraumatic stress disorder; CSF, cerebrospinal fluid; DTI, diffusion tensor imaging.

correlational findings that total cerebral, posterior superior cortical regions and cerebellar gray matter volumes were significantly and negatively correlated with greater number of PTSD symptoms in maltreated youth lend support to this idea. It is possible that less gray matter in these regions attenuates the development of clear memories of the traumatic experiences, leading to impaired processing of traumatic reminders and inability to resolve PTSD symptoms. Less gray matter in maltreatment-related PTSD in these posterior brain areas that are involved in language, vision, visual–spatial skills, emotional and behavioral regulation, and higher cognitive processes may mean less developmentally appropriate neuroconnections and less effective processing of not only trauma stimuli but also all stimuli associated with these brain functions; and may consequently lead to comorbidity and poor overall social outcome. Our significant correlations showing that smaller cerebellar gray matter volumes are associated with higher overall psychopathology scores on the CBCL and lower levels of general function on the CGAS support this idea. In addition, smaller left occipital cortex and fusiform gyrus volumes were seen in youth with PTSD secondary to a variety of trauma types compared with nontraumatized youth (Keding & Herringa, in press). Previous reports have shown smaller cerebellar and vermis volumes in adults with PTSD secondary to interpersonal violence experienced in adulthood compared to adults who were victims of violence who did have PTSD (Baldaçara et al., 2011). Women with a history of childhood sexual abuse had less gray matter in the occipital cortex compared to women with no trauma history (Tomoda et al., 2009).

It is noteworthy that in epidemiological studies, PTSD is commonly associated with other anxiety disorders, depression, externalizing disorders, and greater disease burden (Alonzo,

https://doi.org/10.1017/S0954579415000942 Published online by Cambridge University Press

2000), as was also seen in this pediatric study. Our PTSD subjects had greater rates of separation anxiety disorder, depression, oppositional defiant disorder, and greater number of Axis I disorders than did maltreated youth without chronic PTSD. Because the number of maltreatment types experienced did not correlate with any of the brain differences in this study, it is likely that some maltreated individuals have an inherent vulnerability to PTSD symptoms that occur either prior to, or soon after, severe trauma exposure, which mediates the pathway from chronic PTSD to comorbidity and poor outcome. Our investigation suggests that this vulnerability to chronic PTSD and comorbidity following trauma involves gray matter differences in posterior cortical and cerebellar matter. In support of this idea, adults who suffered from PTSD secondary to a coal mine flood disaster had smaller bilateral calcarine cortex volumes compared to survivors without PTSD; calcarine cortex volumes negatively correlated with greater PTSD symptom severity (Zhang et al., 2011), findings that were similar to this study. In a larger sample of maltreated youth who underwent comprehensive neuropsychological testing, and many of whom were also involved in this study, the PTSD group performed significantly worse than maltreated youth without PTSD on a task in the visuospatial domain that assessed higher order visuoconstructive abilities reflective of intact calcarine and precuneus functioning (De Bellis et al., 2013). Resilient adults with a history of maltreatment demonstrated increased resting-state functional connectivity in the left dorsal anterior cingulate cortex and a larger cluster region containing the bilateral lingual gyrus and the occipital fusiform gyrus compared to both the vulnerable group and the healthy controls (van der Werff et al., 2013). Greater activity in posterior cortex is assumed to be associated with larger brain regions (Schoenemann, 2006).

Compared with maltreated youth without PTSD and controls, maltreated children and adolescents with PTSD had lower axial diffusivity values in the corpus callosum fibers (i.e., splenium) that project to the occipital region of the posterior cortex. In maltreated youth, splenium axial diffusivity significantly and negatively correlated with greater number of PTSD symptoms and significantly and positively correlated with the better global function. However, we did not find decreased fractional anisotropy in the medial and posterior corpus callosum, which was seen in a pilot study of maltreated youth with PTSD compared to controls (Jackowski et al., 2008). Our findings of lower splenium axial diffusivity may indicate early axonal damage (e.g., such as axonal swelling and Wallerian degeneration) in the posterior corpus callosum (Sun et al., 2006). The results of this study may suggest premature development (greater pruning of gray matter along with inflammatory processes directed against the myelin sheath) of the posterior cortex in maltreated youth with PTSD. In support of this idea, elevations of inflammation levels are seen in maltreated children compared to nonmaltreated children (Danese et al., 2009), and adults who were maltreated as children compared to adults without maltreatment histories (Danese, Pariante, Caspi, Taylor, & Poulton, 2007). Furthermore, premature cellular aging as evidenced by telomere shortening were seen in a study of maltreated children (Shalev et al., 2013) and adults maltreated as children (Tyrka et al., 2010), compared to individuals without child maltreatment histories. As opposed to findings of increased fractional anisotropy in adults maltreated during youth (Choi, Jeong, Rohan, Polcari, & Teicher, 2009; Tomoda et al., 2009), in this investigation, we did not see evidence of corpus callosum fractional anisotropy differences in maltreated youth.

Investigations of gender differences and brain maturation in maltreated youth are understudied. In this study, maltreated males with and without PTSD showed less gray matter in left superior prefrontal cortex gray matter (Region 4) compared to maltreated females regardless of PTSD status. There was also a trend for maltreated males with PTSD to show less left superior prefrontal cortex gray matter (Region 4) than male controls. Region 4 includes important structures involved in executive functions, such as the left dorsal medial and lateral prefrontal cortex. These results agree with previous studies that show greater adverse brain development in maltreated boys compared to maltreated girls. In a relatively large pediatric cross-sectional anatomical MRI study, maltreated males with PTSD showed more evidence of adverse brain development (smaller cerebral volumes and larger lateral ventricular volumes) than did maltreated females with PTSD, suggesting sex differences during brain maturation in traumatized youth; this finding was seen even though both boys and girls showed similar psychopathology and trauma histories (De Bellis & Keshavan, 2003). This earlier study did not include a maltreated group without PTSD. A subsequent examination of a subsample from the original study population demonstrated that within 3 years of initial brain scan, 32% of the maltreated males with PTSD but only 5% of the maltreated females with PTSD and none of the controls developed serious antisocial behaviors and suggests less resilience in maltreated males with chronic PTSD (De Bellis & Keshavan, 2003). In an functional MRI study, maltreated boys showed decreased activation in the left prefrontal and posterior cingulate cortex to target detection during fearful face distraction compared to control boys, and maltreated and control girls, while undergoing an emotional oddball task demonstrating that maltreated boys show attention/executive dysfunction secondary to emotional distraction compared to maltreated and nonmaltreated girls and nonmaltreated boys (Crozier, Wang, Huettel, & De Bellis, 2014). Even though in this study, both maltreated boys and girls showed similar psychopathology and trauma histories, these functional MRI results also suggest that there is greater neurobiological vulnerability in maltreated male youth compared to female youth (Crozier et al., 2014). McGloin and Widom (2001) prospectively studied resilience in a large group of adults with substantiated child maltreatment histories and a control group closely matched for age, sex, race, and social class background. In that study, resilience was comprehensively operationalized across eight domains (i.e., employment, homelessness, education, social function, presence of psychiatric disorders and substance abuse, and two measures of antisocial behaviors) and included multiple

https://doi.org/10.1017/S0954579415000942 Published online by Cambridge University Press

assessment waves of their data (McGloin & Widom, 2001). They found maltreated males were lowest on their constructed measure of resilience, thus suggesting increased vulnerability in maltreated males. Taken together, these results suggest greater prefrontal adverse brain development in maltreated males compared to maltreated females, which in turn, may lead to less resilience in maltreated males.

The strengths of our study are as follows. We studied the extremes of psychopathology (chronic PTSD with comorbidity) in relation to global brain structural volumes and corpus callosum microstructure in a group of maltreated youth with an extraordinary level of trauma exposure. Both maltreatment groups suffered a mean of at least five maltreatment types, putting both groups at extremely high risk for adolescent and adult psychopathology and health risk behaviors associated with the leading causes of death in adulthood (Felitti et al., 1998). We recruited healthy and demographically similar groups of maltreated youth involved in CPS and demographically similar nonmaltreated youth, which was a time-consuming task because confounds such as prenatal substance exposure (Besinger et al., 1999; Kelleher et al., 1994; Smith et al., 2007), low SES (Herrenkohl & Herrenkohl, 2007), use of psychotropic medications (Raghavan et al., 2005), and medical illnesses (Hussey et al., 2006; Leslie et al., 2005) are overrepresented in maltreated youth; and each can independently and negatively influence brain maturation. Our inclusion/exclusion procedures were major strengths of our study. Finally, our sample size was sufficient and relatively large for a MRI study in youth involved with CPS, where small sample sizes predominate.

Despite the strengths of our study, a number of limitations are evident. First, both maltreated groups differed from the control group in IQ. This limitation is inherent in child maltreatment studies (De Bellis, 2001b; Perez & Widom, 1994). However, the two maltreatment groups showed very similar means and distributions of IQ scores. Because higher IQ participants demonstrate a linear relationship with neural efficiency compared with lower IQ participants (Neubauer & Fink, 2009), and cortical thickness in this study participants' age and IQ range (average to high average) show linear associations (Shaw et al., 2006), IQ group differences were appropriately addressed using GLM statistical methods. In addition, lower IQ was not associated with PTSD symptoms in the maltreated youth studied here. Second, another limitation is that we were not able to examine age of maltreatment onset in our analyses because maltreated youth had multiple episodes and types of maltreatment experiences. Our data agree with other studies that show that most maltreated children involved in CPS suffered from several types of abuse and neglect (Kaufman et al., 1994). Determining the age of maltreatment onset was not a simple construct because some experiences (e.g., neglect and family violence) were present since birth in most of our maltreated subjects; consequently, measuring this construct was not feasible in this study. Third, our study employed a cross-sectional design, which limits inferences regarding the causality of the group differences seen in anatomical and corpus callosum DTI brain measures. The differences reported in these brain measures may be a shared trauma mechanism that we were unable to measure and may have been present soon after birth (such as a lack of joint attention and/or emotional neglect in infancy) or an inherent vulnerability that mediates the pathway from chronic PTSD to comorbidity that may have been either present prior to the traumas or occurred soon after trauma exposures.

Our study raises questions about the nature of vulnerability (as opposed to resilience) to chronic PTSD in maltreated children and adolescents. Resilience is a complex phenomenon, in which individuals obtain competent functioning despite significant adversity (for a review, see Cicchetti, 2013). The maltreated youth with PTSD showed less competent functioning in the areas of emotional and behavioral regulation, and social skills compared to the two other groups. However, the resilience to PTSD group was not invulnerable: they showed problems in emotional and behavioral regulation, and social skills to a lesser degree. It should also be noted that some subjects in the resilient group had prior PTSD but recovered, suggesting that resilience is not a static concept (Cicchetti, 2013). These ideas lead to the following question: does a threshold of maltreatment exist, above which all maltreated youth vulnerable to chronic PTSD will be found to have decreased gray matter in posterior brain regions, adverse brain development, and poor outcome? Given that this investigation is cross-sectional, we cannot answer this question. The lack of published longitudinal studies in maltreated youth is an impediment in formulating an answer. In our study, total cerebral, posterior superior cortical regions, and cerebellar gray matter volumes significantly and negatively correlated with greater number of PTSD symptoms in maltreated youth. These findings are similar to those shown in earlier studies (De Bellis et al., 1999, 2002; De Bellis & Kuchibhatla, 2006). However, in this study, we did not see any significant or near significant Spearman rho correlations with brain measures and number of maltreatment types experienced except that trauma load was a significant predictor of Region 16 gray matter volume in one of our GML analyses; nor did we see any significant or near significant relationships with PTSD onset or duration. Both maltreatment groups experienced severe traumas. Most subjects in each maltreatment group witnessed intimate partner violence, and experienced neglect and corporal punishment beginning in young childhood.

According to published studies, PTSD symptoms following trauma usually resolve with time (De Bellis & Zisk, 2014). Cross-sectional studies suggest that PTSD prevalence rates in CPS identified maltreated youth are high; 40%–60% of nonclinically referred individuals who have been sexually abused develop PTSD within the 2 months following disclosure (Famularo, Fenton, & Kinscherff, 1993; McLeer et al., 1998). However, follow-up studies demonstrate PTSD symptoms have remitted in half of these children within 2 years (Famularo, Fenton, Augustyn, & Zuckerman, 1996). Thus, the limited published longitudinal data to date suggests that chronic and persistent PTSD symptoms are seen in only 20%–30% of maltreated youth identified by CPS. This rate is similar to the 22% rate of resilience as defined by McGloin

https://doi.org/10.1017/S0954579415000942 Published online by Cambridge University Press

and Widom (2001) as seen in adults who were followed in a longitudinal study of maltreated youth and similar to the resiliency rates in maltreated youth and adults as described in a critical review by Cicchetti (2013). These adults (McGloin & Widom, 2001) were not assessed for PTSD during childhood; however, these subjects did suffer from high rates of PTSD in adulthood (which ranged from rates of PTSD of 30.6% for neglect victims to 37.5% for sexual abuse victims; Widom, 1999). Taken together, the results of all these investigations lend to the speculation that chronic and persistent PTSD leads to comorbidity and poor outcome; however, to the best of our knowledge, this hypothesis has not been tested in a longitudinal study.

According to experts in operant conditioning theory, PTSD is considered to be a disorder of recovery, in which individuals who suffer from trauma fail to learn extinction and extinction retention of the fear response elicited by traumatic reminders (Pitman et al., 2012; Yehuda & LeDoux, 2007). Extinction is an active process of acquiring and maintaining new learning (Milad & Quirk, 2012). The key brain structures involved in these processes (amygdala, hippocampus, anterior cingulate cortex, and ventral medial prefrontal cortex) are located in cortical parcellation regions in which we did not see significant differences between groups using this method. However, we did see volumetric differences in gray matter in the posterior cortex and cerebellum, whose functions are also involved in fear conditioning as well as behavioral, cognitive, and emotional regulation.

An inherent difficulty in diagnosis of PTSD is the lack of an answer to the empirical question of whether failure to recover from PTSD symptoms is a shared mechanism in which vulnerable individuals have deficits in not only fear but also other neural pathways that control behavioral, cognitive, and emotional regulation (which may lead to adverse brain development and poor outcome). PTSD from maltreatment is a social trauma. Therefore, the diagnosis is best made by a pediatric clinician who is informed about the manifestations of pediatric trauma but also trained in the recognition of developmental and social nuances of expression of maltreatment-related traumatic reminders during different developmental periods (American Academy of Child and Adolescent Psychiatry, 2010). This type of research assessment is extremely difficult to perform during a one-time child and parent structured interview. In a structured (as opposed to semistructured) interview without a trauma-informed interviewer, a maltreated child is likely to shut down and avoid trauma issues. This fact may explain the low rates of PTSD despite high rates and risk for disorders (e.g., depressive and generalized anxiety disorders) that have symptoms in common with PTSD, and seen in youth with trauma histories in both cross-sectional (Kilpatrick et al., 2003) and longitudinal (Copeland, Keeler, Angold, & Costello, 2007) pediatric epidemiological studies using structured interviews.

Longitudinal work in pediatric PTSD benefits from the relationship between the study center (e.g., university-based trauma programs and summer camps with university-educated clinical researchers) and the affected youth. Longitudinal work that involves neuroimaging, biological markers, evidenced-based interventions, and treatments to determine if plasticity is present and recovery of brain structure and function are occurring is paramount and requires a center with expert neuroscientists and trauma-informed clinicians. To prevent the grave societal and human consequences of maltreatment, it is imperative that our society begin to plan for these types of multisite longitudinal studies in both at-risk mothers to be and maltreated youth. This type of infrastructure can be designed to be informative in studying both the neurobiology of prevention of maltreatment and the developmental medical and mental health consequences of trauma.

In summary, we successfully identified volumetric differences in brain structures associated with behavioral, cognitive, and emotional regulation (i.e., the posterior cerebral and cerebellar gray matter brain volumes and DTI differences in the splenium of the corpus callosum) between maltreated youth with chronic PTSD and those resilient to chronic PTSD. Alterations of these structures may result from a shared trauma-related mechanism or an inherent vulnerability that mediates the pathway from chronic PTSD to comorbidity. These data advance the field by providing evidence that cortical differences and microstructural differences in the corpus callosum are seen in pediatric maltreatment-related chronic PTSD, early in the development of this illness. Posterior brain regions are associated with the successful attainment of age-appropriate emotional, behavioral, and cognitive regulation. Longitudinal research is needed to determine whether the neurobiology associated with PTSD becomes a shared mechanism for disorders that reflect impaired emotional, behavioral, and cognitive regulation and decision making, such as depression and substance use disorders, in adolescents and adulthood, and if the neurobiology of resilience to chronic PTSD following severe maltreatment is a marker for healthier adulthood adaptations to childhood trauma. Further longitudinal work is also needed to determine neurobiological factors related to chronic and persistent PTSD, and to PTSD resilience despite maltreatment.

References

Alonzo, A. A. (2000). The experience of chronic illness and post-traumatic stress disorder: The consequences of cumulative adversity. *Social Science & Medicine*, *50*, 1475–1484.

American Academy of Child and Adolescent Psychiatry. (2010). Practice parameter for the assessment and treatment of children and adolescents with posttraumatic stress disorder. *Journal of the American Academy of Child & Adolescent Psychiatry*, *49*, 414–430.

Asato, M. R., Terwilliger, R., Woo, J., & Luna, B. (2010). White matter development in adolescence: A DTI study. *Cerebral Cortex*, *20*, 2122–2131.

https://doi.org/10.1017/S0954579415000942 Published online by Cambridge University Press

Baldaçara, L., Jackowski, A. P., Schoedl, A., Pupo, M., Andreoli, S. B., Mello, M. F., et al. (2011). Reduced cerebellar left hemisphere and vermal volume in adults with PTSD from a community sample. *Journal of Psychiatric Research*, *45*, 1627–1633.

Bauer, P. M., Hanson, J. L., Pierson, R. K., Davidson, R. J., & Pollak, S. D. (2009). Cerebellar volume and cognitive functioning in children who experienced early deprivation. *Biological Psychiatry*, *66*, 1100–1106.

Bellebaum, C., & Daum, I. (2007). Cerebellar involvement in executive control. *Cerebellum*, *6*, 184–192.

Besinger, B., Garland, A. F., Litrownik, A. J., & Landsverk, J. A. (1999). Caregiver substance abuse among maltreated children placed in out-of-home care. *Child Welfare*, *78*, 221–239.

Beyer, J. L., Kuchibhatla, M., Payne, M. E., MacFall, J., Cassidy, F., & Krishnan, K. R. R. (2009). Gray and white matter brain volumes in older adults with bipolar disorder. *International Journal of Geriatric Psychiatry*, *24*, 1445–1452.

Bucker, J., Muralidharan, K., Torres, I. J., Su, W., Kozicky, J., Silveira, L. E., et al. (2014). Childhood maltreatment and corpus callosum volume in recently diagnosed patients with bipolar I disorder: Data from the Systematic Treatment Optimization Program for Early Mania (STOP-EM). *Journal of Psychiatric Research*, *48*, 65–72.

Carrion, V. G., Weems, C. F., Eliez, S., Patwardhan, A., Brown, W., Ray, R. D., et al. (2001). Attenuation of frontal asymmetry in pediatric posttraumatic stress disorder. *Biological Psychiatry*, *50*, 943–951.

Carrion, V. G., Weems, C. F., Watson, C., Eliez, S., Menon, V., & Reiss, A. L. (2009). Converging evidence for abnormalities of the prefrontal cortex and evaluation of midsagittal structures in pediatric posttraumatic stress disorder: An MRI study. *Psychiatry Research: Neuroimaging*, *172*, 226–234.

Cavanna, A. E., & Trimble, M. R. (2006). The precuneus: A review of its functional anatomy and behavioural correlates. *Brain*, *129*, 564–583.

Chiang, M.-C., McMahon, K. L., de Zubicaray, G. I., Martin, N. G., Hickie, I., Toga, A. W., et al. (2011). Genetics of white matter development: A DTI study of 705 twins and their siblings aged 12 to 29. *NeuroImage*, *54*, 2308–2317.

Choi, J., Jeong, B., Rohan, M. L., Polcari, A., & Teicher, M. H. (2009). Preliminary evidence for white matter tract abnormalities in young adults exposed to parental verbal abuse. *Biological Psychiatry*, *65*, 227–234.

Cicchetti, D. (2013). Annual Research Review: Resilient functioning in maltreated children—Past, present, and future perspectives. *Journal of Child Psychology and Psychiatry*, *54*, 402–422.

Cirulli, F., Francia, N., Berry, A., Aloe, L., Alleva, E., & Suomi, S. J. (2009). Early life stress as a risk factor for mental health: Role of neurotrophins from rodents to non-human primates. *Neuroscience & Biobehavioral Reviews*, *33*, 573–585.

Cohen, R. A., Grieve, S., Hoth, K. F., Paul, R. H., Sweet, L., Tate, D., et al. (2006). Early life stress and morphometry of the adult anterior cingulate cortex and caudate nuclei. *Biological Psychiatry*, *59*, 975–982.

Copeland, W., Keeler, G., Angold, A., & Costello, E. (2007). Traumatic events and posttraumatic stress in childhood. *Archives of General Psychiatry*, *64*, 577–584.

Crozier, J. C., Wang, L., Huettel, S. A., & De Bellis, M. D. (2014). Neural correlates of cognitive and affective processing in maltreated youth with posttraumatic stress symptoms: Does gender matter? *Development and Psychopathology*, *26*, 491–513.

Damasio, H. (1995). *Human brain anatomy in computerized images*. New York: Oxford University Press.

Danese, A., Moffitt, T. E., Harrington, H., Milne, B. J., Polanczyk, G., Pariante, C. M., et al. (2009). Adverse childhood experiences and adult risk factors for age-related disease: Depression, inflammation, and clustering of metabolic risk markers. *Archives of Pediatrics and Adolescent Medicine*, *163*, 1135–1143.

Danese, A., Pariante, C. M., Caspi, A., Taylor, A., & Poulton, R. (2007). Childhood maltreatment predicts adult inflammation in a life-course study. *Proceedings of the National Academy of Sciences*, *104*, 1319–1324.

Dannlowski, U., Stuhrmann, A., Beutelmann, V., Zwanzger, P., Lenzen, T., Grotegerd, D., et al. (2012). Limbic scars: Long-term consequences of childhood maltreatment revealed by functional and structural magnetic resonance imaging. *Biological Psychiatry*, *71*, 286–293.

De Bellis, M. D. (2001a). Developmental traumatology: A contributory mechanism for alcohol and substance use disorders. Special Review. *Psychoneuroendocrinology*, *27*, 155–170.

De Bellis, M. D. (2001b). Developmental traumatology: The psychobiological development of maltreated children and its implications for research, treatment, and policy. *Development and Psychopathology*, *13*, 539–564.

De Bellis, M. D., Hooper, S., Spratt, E. G., & Woolley, D. W. (2009). Neuropsychological findings in childhood neglect and their relationships to pediatric PTSD. *Journal of the International Neuropsychological Society*, *15*, 868–878.

De Bellis, M. D., & Keshavan, M. S. (2003). Sex differences in brain maturation in maltreatment-related pediatric posttraumatic stress disorder. *Neuroscience & Biobehavioral Reviews*, *27*, 103–117.

De Bellis, M. D., Keshavan, M. S., Beers, S. R., Hall, J., Frustaci, K., Masalehdan, A., et al. (2001). Sex differences in brain maturation during childhood and adolescence. *Cerebral Cortex*, *11*, 552–557.

De Bellis, M. D., Keshavan, M., Clark, D. B., Casey, B. J., Giedd, J., Boring, A. M., et al. (1999). A. E. Bennett Research Award. Developmental Traumatology: Part II. Brain Development. *Biological Psychiatry*, *45*, 1271–1284.

De Bellis, M. D., Keshavan, M., Shifflett, H., Iyengar, S., Beers, S. R., Hall, J., et al. (2002). Brain structures in pediatric maltreatment-related posttraumatic stress disorder: A sociodemographically matched study. *Biological Psychiatry*, *52*, 1066–1078.

De Bellis, M., & Kuchibhatla, M. (2006). Cerebellar volumes in pediatric maltreatment-related posttraumatic stress disorder. *Biological Psychiatry*, *60*, 697–703.

De Bellis, M. D., Narasimhan, A., Thatcher, D. L., Keshavan, M. S., Soloff, P., & Clark, D. B. (2005). Prefrontal cortex, thalamus and cerebellar volumes in adolescents and young adults with adolescent onset alcohol use disorders and co-morbid mental disorders *Alcoholism: Clinical and Experimental Research*, *29*, 1590–1600.

De Bellis, M. D., Woolley, D. P., & Hooper, S. R. (2013). Neuropsychological findings in pediatric maltreatment: Relationship of PTSD, dissociative symptoms, and abuse/neglect indices to neurocognitive outcomes. *Child Maltreatment*, *18*, 171–183.

De Bellis, M. D., & Zisk, A. (2014). The biological effects of childhood trauma. *Child and Adolescent Psychiatric Clinics of North America: Disaster and Trauma*, *23*, 185–222.

Devlin, J. T., Jamison, H. L., Gonnerman, L. M., & Matthews, P. M. (2006). The role of the posterior fusiform gyrus in reading. *Journal of Cognitive Neuroscience*, *18*, 911–922.

Dougherty, R. F., Koch, V. M., Brewer, A. A., Fischer, B., Modersitzki, J., & Wandell, B. A. (2003). Visual field representations and locations of visual areas V1/2/3 in human visual cortex. *Journal of Vision*, *3*, 586–598.

Famularo, R., Fenton, T., Augustyn, M., & Zuckerman, B. (1996). Persistence of pediatric post traumatic stress disorder after 2 years. *Child Abuse & Neglect*, *20*, 1245–1248.

Famularo, R., Fenton, T., & Kinscherff, R. (1993). Child maltreatment and the development of post traumatic stress disorder. *American Journal of Diseases of Children*, *147*, 755–760.

Felitti, V. J., Anda, R. F., Nordenberg, D., Williamson, D. F., Spitz, A. M., Edwards, V., et al. (1998). Relationship of childhood abuse and household dysfunction to many of the leading causes of death in adults. *American Journal of Preventive Medicine*, *14*, 245–258.

Fransson, P. (2006). How default is the default mode of brain function? Further evidence from intrinsic BOLD signal fluctuations. *Neuropsychologia*, *44*, 2836–2845.

Giedd, J. N., & Rapoport, J. L. (2010). Structural MRI of pediatric brain development: What have we learned and where are we going? *Neuron*, *67*, 728–734.

Giuliani, N. R., Calhoun, V. D., Pearlson, G. D., Francis, A., & Buchanan, R. W. (2005). Voxel-based morphometry versus region of interest: A comparison of two methods for analyzing gray matter differences in schizophrenia. *Schizophrenia Research*, *74*, 135–147.

Hagmann, P., Cammoun, L., Martuzzi, R., Maeder, P., Clarke, S., Thiran, J.-P., et al. (2006). Hand preference and sex shape the architecture of language networks. *Human Brain Mapping*, *27*, 828–835.

Hanson, J. L., Chung, M. K., Avants, B. B., Shirtcliff, E. A., Gee, J. C., Davidson, R. J., et al. (2010). Early stress is associated with alterations in the orbitofrontal cortex: A tensor based morphometry investigation of brain structure and behavioral risk. *Journal of Neuroscience*, *30*, 7466–7472.

Herrenkohl, T. I., & Herrenkohl, R. C. (2007). Examining the overlap and prediction of multiple forms of child maltreatment, stressors, and socioeconomic status: A longitudinal analysis of youth outcomes. *Journal of Family Violence*, *22*, 553–562.

Huang, H., Zhang, J., Jiang, H., Wakana, S., Poetscher, L., Miller, M. I., et al. (2005). DTI tractography based parcellation of white matter: Application

https://doi.org/10.1017/S0954579415000942 Published online by Cambridge University Press

to the mid-sagittal morphology of corpus callosum. *NeuroImage*, *26*, 195–205.
Hussey, J. M., Chang, J. J., & Kotch, J. B. (2006). Child maltreatment in the United States: Prevalence, risk factors, and adolescent health consequences. *Pediatrics*, *118*, 933–942.
Isabelle, K., Paradis, A.-L., Poline, J.-B., Kosslyn, S. M., & Denis Le Bihan, D. (2000). Transient activity in the human calcarine cortex during visual-mental imagery: An event-related fMRI study. *Journal of Cognitive Neuroscience*, *12*(Suppl. 2), 15–23.
Jackowski, A. P., Douglas-Palumberi, H., Jackowski, M., Win, L., Schultz, R. T., Staib, L. W., et al. (2008). Corpus callosum in maltreated children with posttraumatic stress disorder: A diffusion tensor imaging study. *Psychiatry Research: Neuroimaging*, *162*, 256–261.
Kaufman, J., Birmaher, B., Brent, D., Rao, U., Flynn, C., Moreci, P., et al. (1997). Schedule for Affective Disorders and Schizophrenia for School-Age Children—Present and lifetime version (K-SADS-PL): Initial reliability and validity data. *Journal of the American Academy of Child & Adolescent Psychiatry*, *36*, 980–988.
Kaufman, J., Jones, B., Stieglitz, E., Vitulano, L., & Mannarino, A. (1994). The use of multiple informants to assess children's maltreatment experiences. *Journal of Family Violence*, *9*, 227–248.
Keding, T. J., & Herringa, R. J. (in press). Abnormal structure of fear circuitry in pediatric post-traumatic stress disorder. *Neuropsychopharmacology.*
Kelleher, K., Chaffin, M., Hollenberg, J., & Fischer, E. (1994). Alcohol and drug disorders among physically abusive and neglectful parents in a community-based sample. *American Journal of Public Health*, *84*, 1586–1590.
Kelly, P. A., Viding, E., Wallace, G. L., Schaer, M., De Brito, S. A., Robustelli, B., et al. (2013). Cortical thickness, surface area, and gyrification abnormalities in children exposed to maltreatment: Neural markers of vulnerability? *Biological Psychiatry*, *74*, 845–852.
Kilpatrick, D. G., Ruggiero, K. J., Acierno, R., Saunder, B., Resnick, H. S., & Best, C. L. (2003). Violence and risk of PTSD, major depression, substance abuse/dependence, and comorbidity: Results From the National Survey of Adolescents. *Journal of Consulting and Clinical Psychology*, *71*, 692–700.
Kitayama, N., Brummer, M., Hertz, L., Quinn, S., Kim, Y., & Bremner, J. D. (2007). Morphologic alterations in the corpus callosum in abuse-related posttraumatic stress disorder: A preliminary study. *Journal of Nervous and Mental Disease*, *195*, 1027–1029.
Kitayama, N., Quinn, S., & Bremner, J. D. (2006). Smaller volume of anterior cingulate cortex in abuse-related posttraumatic stress disorder. *Journal of Affective Disorders*, *90*, 171–174.
Kubicki, M., Shenton, M. E., Salisbury, D. F., Hirayasu, Y., Kasai, S. K., Kikinis, R., et al. (2002). Voxel-based morphometric analysis of gray matter in first episode schizophrenia. *NeuroImage*, *17*, 1711–1719.
Lange, N., Froimowitz, M. P., Bigler, E. D., Lainhart, J. E., & Brain Development Cooperative Group. (2010). Associations between IQ, total and regional brain volumes, and demography in a large normative sample of healthy children and adolescents. *Developmental Neuropsychology*, *35*, 296–317.
Lebel, C., & Beaulieu, C. (2011). Longitudinal development of human brain wiring continues from childhood into adulthood. *Journal of Neuroscience*, *31*, 10937–10947.
Lebel, C., Caverhill-Godkewitsch, S., & Beaulieu, C. (2010). Age-related regional variations of the corpus callosum identified by diffusion tensor tractography. *NeuroImage*, *52*, 20–31.
Leslie, L. K., Gordon, J. N., Meneken, L., Premji, K., Michaelmore, K. L., & Ganger, W. (2005). The physical, developmental, and mental health needs of young children in child welfare by initial placement type. *Developmental and Behavioral Pediatrics*, *26*, 177–185.
Maes, F., Collignon, A., Vandermeulen, D., Marchal, G., & Suetens, P. (1997). Multimodality image registration by maximization of mutual information. *IEEE Transactions on Medical Imaging*, *16*, 187–198.
McGloin, J. M., & Widom, C. S. (2001). Resilience among abused and neglected children grown up. *Development and Psychopathology*, *13*, 1021–1038.
McLeer, S. V., Dixon, J. F., Henry, D., Ruggiero, K., Escovitz, K., Niedda, T., et al. (1998). Psychopathology in non-clinically referred sexually abused children. *Journal of the American Academy of Child & Adolescent Psychiatry*, *37*, 1326–1333.
Milad, M. R., & Quirk, G. J. (2012). Fear extinction as a model for translational neuroscience: Ten years of progress. *Annual Review Psychology*, *62*, 129–151.
Neubauer, A. C., & Fink, A. (2009). Intelligence and neural efficiency. *Neuroscience & Biobehavioral Reviews*, *33*, 1004–1023.
Perez, C., & Widom, C. S. (1994). Childhood victimization and long-term intellectual and academic outcomes. *Child Abuse & Neglect*, *18*, 617–633.
Pitman, R. K., Rasmusson, A. M., Koenen, K. C., Shin, L. M., Orr, S. P., Gilbertson, M. W., et al. (2012). Biological studies of post-traumatic stress disorder. *Nature Reviews: Neuroscience*, *13*, 769–787.
Prochnowa, D., Kossacka, H., Brunheima, S. K., Müllera, K., Wittsackb, H.-J., Markowitschc, H.-J., et al. (2013). Processing of subliminal facial expressions of emotion: A behavioral and fMRI study. *Social Neuroscience*, *8*, 448–461. doi:10.1080/17470919.2013.812536
Raghavan, R., Zima, B. T., Andersen, R. M., Leibowitz, A. A., Schuster, M. A., & Landsverk, J. (2005). Psychotropic medication use in a national probability sample of children in the child welfare system. *Journal of Child and Adolescent Psychopharmacology*, *15*, 97–106.
Riva, D., & Giorgi, C. (2000). The cerebellum contributes to higher functions during development. *Brain*, *123*, 1051–1061.
Rothman, K. J. (1990). No adjustments are needed for multiple comparisons. *Epidemiology*, *1*, 43–46.
Sacchetti, B., Scelfo, B., Tempia, F., & Strata, P. (2004). Long-term synaptic changes induced in the cerebellar cortex by fear conditioning. *Neuron*, *42*, 973–982.
Sanchez, M. M., Hearn, E. F., Do, D., Rilling, J. K., & Herndon, J. G. (1998). Differential rearing affects corpus callosum size and cognitive function of rhesus monkeys. *Brain Research*, *812*, 38–49.
Sandor, S., & Leahy, R. (1997). Surface-based labeling of cortical anatomy using a deformable database. *IEEE Transactions on Medical Imaging*, *16*, 41–54.
Satterthwaite, T. D., Vandekar, S., Wolf, D. H., Ruparel, K., Roalf, D. R., Jackson, C., et al. (2014). Sex differences in the effect of puberty on hippocampal morphology. *Journal of the American Academy of Child & Adolescent Psychiatry*, *53*, 341–350.
Schoenemann, P. T. (2006). Evolution of the size and functional areas of the human brain. *Annual Review of Anthropology*, *35*, 379–406.
Schutter, D. J. L. G., & van Honk, J. (2005). The cerebellum on the rise in human emotion. *Cerebellum*, *4*, 290–294.
Sehlmeyer, C., Schöning, S., Zwitserlood, P., Pfleiderer, B., Kircher, T., Arolt, V., et al. (2009). Human fear conditioning and extinction in neuroimaging: A systematic review. *PLOS ONE*, *4*, e5865.
Shaffer, D., Gould, M. S., Brasic, J., Ambrosini, P., Fisher, P., Bird, H., et al. (1983). A children's global assessment scale. *Archives of General Psychiatry*, *40*, 1228–1231.
Shalev, I., Moffitt, T. E., Sugden, K., Williams, B., Houts, R. M., Danese, A., et al. (2013). Exposure to violence during childhood is associated with telomere erosion from 5 to 10 years of age: A longitudinal study. *Molecular Psychiatry*, *18*, 576–581.
Shattuck, D. W., & Leahy, R. M. (2001). Graph based analysis and correction of cortical volume topology. *IEEE Transactions on Medical Imaging*, *20*, 1167–1177.
Shattuck, D. W., Sandor-Leahy, S. R., Schaper, K. A., Rottenberg, D. A., & Leahy, R. (2001). Magnetic resonance image tissue classification using a partial volume model. *NeuroImage*, *13*, 856–876.
Shaw, P., Greenstein, D., Lerch, J., Clasen, L., Lenroot, R., Gogtay, N., et al. (2006). Intellectual ability and cortical development in children and adolescents. *Nature Letters*, *440*, 676–679.
Smith, D. K., Johnson, A. B., Pears, K. C., Fisher, P. A., & DeGarmo, D. S. (2007). Child maltreatment and foster care: Unpacking the effects of prenatal and postnatal parental substance use. *Child Maltreatment*, *12*, 150.
Smith, S. M. (2002). Fast robust automated brain extraction. *Human Brain Mapping*, *17*, 143–155.
Solomon, S. G., & Rosa, M. G. P. (2014). A simpler primate brain: The visual system of the marmoset monkey. *Frontiers in Neura Circuits*, *8*, 1–24.
Sun, S.-W., Liang, H.-F., Trinkaus, K., Cross, A. H., Armstrong, R. C., & Song, S.-K. (2006). Noninvasive detection of cuprizone induced axonal damage and demyelination in the mouse corpus callosum. *Magnetic Resonance in Medicine*, *55*, 302–308.
Teicher, M. H., Anderson, C. M., & Polcari, A. (2012). Childhood maltreatment is associated with reduced volume in the hippocampal subfields CA3, dentate gyrus, and subiculum. *Proceedings of the National Academy of Sciences*, *109*, E563–E572.
Teicher, M. H., Dumont, N. L., Ito, Y., Vaituzis, C., Giedd, J. N., & Andersen, S. L. (2004). Childhood neglect is associated with reduced corpus callosum area. *Biological Psychiatry*, *56*, 80–85.

https://doi.org/10.1017/S0954579415000942 Published online by Cambridge University Press

Thoma, P., Bellebaum, C., Koch, B., Schwarz, M., & Daum, I. (2008). The cerebellum is involved in reward-based reversal learning. *Cerebellum*, *7*, 433–443.

Thomaes, K., Dorrepaal, E., Draijer, N., de Ruiter, M. B., van Balkom, A. J., Smit, J. H., et al. (2010). Reduced anterior cingulate and orbitofrontal volumes in child abuse-related complex PTSD. *Journal of Clinical Psychiatry*, *71*, 1636–1644.

Tomoda, A., Suzuki, H., Rabi, K., Sheu, Y.-S., Polcari, A., & Teicher, M. H. (2009). Reduced prefrontal cortical gray matter volume in young adults exposed to harsh corporal punishment. *NeuroImage*, *47*, T66–T71.

Tyrka, A. R., Price, L. H., Kao, H.-T., Porton, B., Marsella, S. A., & Carpenter, L. L. (2010). Childhood Maltreatment and telomere shortening: Preliminary support for an effect of early stress on cellular aging. *Biological Psychiatry*, *67*, 531–534.

van der Werff, S. J., Pannekoek, J. N., Veer, I. M., van Tol, M. J., Aleman, A., Veltman, D. J., et al. (2013). Resilience to childhood maltreatment is associated with increased resting-state functional connectivity of the salience network with the lingual gyrus. *Child Abuse & Neglect*, *37*, 1021–1029.

van Harmelen, A.-L., van Tol, M.-J., van der Wee, N. J. A., Veltman, D. J., Aleman, A., Spinhoven, P., et al. (2010). Reduced medial prefrontal cortex volume in adults reporting childhood emotional maltreatment. *Biological Psychiatry*, *68*, 832–838.

Van Leemput, K., Maes, F., Vandermeulen, D., Colchester, A., & Suetens, P. (2001). Automated segmentation of multiple sclerosis lesions by model outlier detection. *IEEE Transactions on Medical Imaging*, *20*, 677–688.

Van Leemput, K., Maes, F., Vandermeulen, D., & Suetens, P. (2003). A unifying framework for partial volume segmentation of brain MR images. *IEEE Transactions on Medical Imaging*, *22*, 105–119.

Villarreal, G., Hamilton, D. A., Graham, D. P., Driscoll, I., Qualls, C., Petropoulos, H., et al. (2004). Reduced area of the corpus callosum in posttraumatic stress disorder. *Psychiatry Research: Neuroimaging*, *131*, 227–235.

Wechsler, D. (1991). *Wechsler Intelligence Scale for Children* (3rd ed.). San Antonio, TX: Psychological Corporation.

Widom, C. S. (1999). Posttraumatic stress disorder in abused and neglected children grown up. *American Journal of Psychiatry*, *156*, 1223–1229.

Yehuda, R., & LeDoux, J. E. (2007). Response variation following trauma: A translational neuroscience approach to understanding PTSD. *Neuron*, *56*, 19–32.

Yoo, T. S., Ackerman, M. J., Lorensen, W. E., Schroeder, W., Chalana, V., Aylward, S., et al. (2002). Engineering and algorithm design for an image processing API: A technical report on ITK—The Insight Toolkit. In J. Westwood (Ed.), *Proceedings of medicine meets virtual reality* (pp. 586–592). Amsterdam: IOS Press.

Yushkevich, P. A., Piven, J., Hazlett, H. C., Smith, R. G., Ho, S., Gee, J. C., et al. (2006). User-guided 3D active contour segmentation of anatomical structures: Significantly improved efficiency and reliability. *NeuroImage*, *31*, 1116–1128.

Zhang, J., Tan, Q., Yin, H., Zhang, X., Huan, Y., Tang, L., et al. (2011). Decreased gray matter volume in the left hippocampus and bilateral calcarine cortex in coal mine flood disaster survivors with recent onset PTSD. *Psychiatry Research: Neuroimaging*, *192*, 84–90.

Zhang, L.-X., Levine, S., Dent, G., Zhan, G., Xing, G., Okimoto, D., et al. (2002). Maternal deprivation increases cell death in the infant rat brain. *Developmental Brain Research*, *133*, 1–11.

https://doi.org/10.1017/S0954579415000942 Published online by Cambridge University Press